RL-TR-92-81
Final Technical Report
May 1992

HIGH SENSITIVITY PROBES FOR SILICON VLSI INTERNAL NODE TESTING

University of Michigan

Janis A. Valdmanis

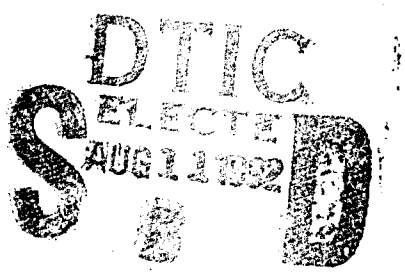

APPROVED FOR PUBLIC RELEASE; DISTRIBUTION UNLIMITED.

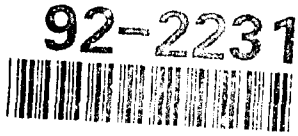

Rome Laboratory
Air Force Systems Command
Griffiss Air Force Base, NY 13441-5700

REPORT DOCUMENTATION PAGE

Form Approved
OMB No. 0704-0188

1. AGENCY USE ONLY (Leave Blank)	2. REPORT DATE	3. REPORT TYPE AND DATES COVERED
	May 1992	Final Sep 89 - Sep 91

4. TITLE AND SUBTITLE

HIGH SENSITIVITY PROBES FOR SILICON VLSI INTERNAL NODE TESTING

5. FUNDING NUMBERS

C - F30602-88-D-0028
N-9-5704
PE - 62702F
PR - 2338
TA - 01
WU - PW

6. AUTHOR(S)

Janis A. Valdmanis

7. PERFORMING ORGANIZATION NAME(S) AND ADDRESS(ES)

University of Michigan
Ultrafast Science Laboratory
2200 Bonisteel Drive
Ann Arbor MI 48109-2099

8. PERFORMING ORGANIZATION REPORT NUMBER

9. SPONSORING/MONITORING AGENCY NAME(S) AND ADDRESS(ES)

Rome Laboratory (ERDR)
Griffiss AFB NY 13441-5700

10. SPONSORING/MONITORING AGENCY REPORT NUMBER

RL-TR-92-81

11. SUPPLEMENTARY NOTES

Rome Laboratory Project Engineer: Daniel J Burns/ERDR/315-330-2868
Prime Contractor: University of Dayton (USAF Expert Science & Engineering Program)

12a. DISTRIBUTION/AVAILABILITY STATEMENT

Approved for public release; distribution unlimited.

12b. DISTRIBUTION CODE

13. ABSTRACT (Maximum 200 words)

This contract investigated several new technologies useful for real-time internal node probing of VLSI integrated circuits. Electro-optic, electroabsorptive, photo-conductive, and magnetic probe technologies were studied, and their relative merits and drawbacks compared. Testing parameters were $\lesssim$ 5ns temporal resolution, $\leq$ 50 mV sensitivity, and $\leq$ 2 spatial resolution. Both theoretical and experimental work was performed. Conclusions are drawn indicating the most promising candidates for future in-depth studies.

14. SUBJECT TERMS

Integrated circuit testing; opto-electronics; circuit probing; high-speed

15. NUMBER OF PAGES

64

16. PRICE CODE

17. SECURITY CLASSIFICATION OF REPORT	18. SECURITY CLASSIFICATION OF THIS PAGE	19. SECURITY CLASSIFICATION OF ABSTRACT	20. LIMITATION OF ABSTRACT
UNCLASSIFIED	UNCLASSIFIED	UNCLASSIFIED	UL

Table of Contents

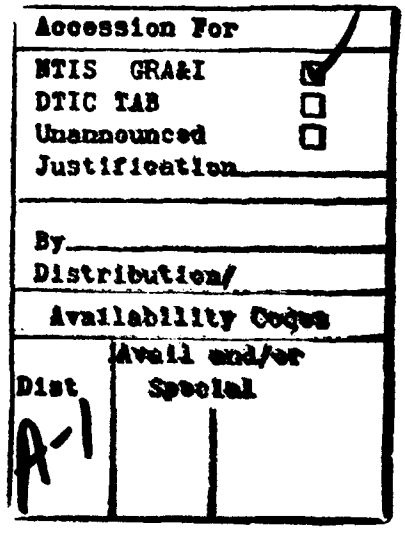

High-sensitivity probes for silicon VLSI internal node testing

I. Introduction

The objective of this work was to investigate a new class of probe for the testing of internal nodes of integrated circuits, primarily silicon. Because the main aim was silicon VLSI, there were particular features of the probes that needed to be addressed. Although the temporal resolution requirements were relatively low, i.e. only less than 5 ns, the spatial resolution requirements, on the other hand, were reasonably stringent, i.e. less than about 2 μm. The sensitivity needed was typical for digital IC's, where a reasonable signal to noise ratio could be achieved with a noise level of roughly 50 mV.

Standard, all electronic, IC probes, as commonly found on IC probe stations, could attain the 5 ns temporal resolution, but not at internal nodes. Internal node probing imposes the requirements of a very small active tip and the ability to probe the active signal without loading the circuit. This would normally mean a high-impedance probe, but that usually carries with it the burden of slow response times.

This study was to look at the use of high-speed opto-electronic techniques as an alternative to all electronic systems. Nanosecond speeds, although fast in electrical systems are relatively easy to achieve in optical systems where picosecond response times are commonplace.

The techniques explored in this study are a direct result of the great success that the techniques of electro-optic (E-O) sampling and photoconductive (P-C) sampling [1] have had in recent years. These are both extremely high impedance type techniques that offer the superior temporal performance associated with optical sampling gates. E-O sampling has been, and still is, the fastest way (in terms of temporal resolution) of measuring repetitive electrical signals. Its subpicosecond performance, as well as its capabiltiy of probing internal nodes, has been investigated by many groups in many material systems and hence is well documented. The main drawback of E-O sampling up to now, however, has been its lack of sensitivity which has made it difficult to use in small signal applications. P-C sampling, which in general has better sensitivity, has also penetrated the subpicosecond regime with the advent of new MBE grown materials for use as sampling gates, e.g. LT GaAs. However, P-C sampling requires contact with the circuit, which is another point of contention. These long-established techniques have not really been adapted to the slower, higher sensitivity needs of silicon IC probing as of yet. In many cases, it is entirely possible to make trade-offs to enhance sensitivity at the expense of temporal performance. This is what we have concentrated on, and describe in the following sections.

It should be noted there are three main components to this type of probe, the tip itself (where it either contacts the circuit or interacts with the local fields), the transducer component, which in large part determines the speed and sensitivity of the probe as a whole, and the mechanism for transmitting the sampled information out to the processing and display electronics. This work limits its scope to the performance of the transducer element, since this is the most important element in the system. There is currently other AFOSR sponsored work going on in the laboratories at USL where new, high resolution tips are being investigated [S. Williamson, PI].

We have examined four main types of transducer that could potentially be used for either contacting or non-contacting applications. These are: a bulk lithium tantalate fabry-perot modulator, a MQW Fabry-Perot electro-absorption modulator, a new type of magnetic field probe, and a photoconductive sampling probe. Each of these will be discussed individually in the next sections.

II. Bulk electro-optic Fabry-Perot probes

A. Introduction

Electro-optic probing techniques are currently the fastest methods of measuring electrical waveforms in a wide variety of electronic geometries. However, there is great interest in being able to probe *internal* points of integrated circuits in order to characterize device and circuit operation in situ. With this aim, two methods of e-o sampling have emerged as powerful techniques for probing internal nodes of IC's. One specialized arrangement was developed to perform sampling directly in the substrate of, specifically, GaAs integrated circuits. Because GaAs is E-O, almost any internal point of the circuit could be accessed. However, GaAs is the only commonly used semiconducting material that is also E-O. The substrate probing technique, or *internal* E-O sampling, also requires the surfaces of the integrated circuit to be of optical quality and the sampling laser beam to have a photon energy below the band gap energy of the substrate material.

Ideally one would like a non-perturbative means of probing integrated circuits with high temporal and spatial resolution that is generally applicable to circuits fabricated on any type of substrate, especially silicon. We have developed and demonstrated a new, non-contact, picosecond, E-O technique for probing internal nodes of high speed integrated circuits fabricated on any substrate material. This technique, referred to as *external* E-O sampling, has demonstrated subpicosecond temporal resolution, micron spatial resolution, and is designed to operate at the wafer level with conventional wafer probing equipment without any special circuit preparation. Optical pulses from any picosecond, high repetition rate laser throughout the visible and near infrared can be used. A similar system, employing a GaAs injection laser, has also been

demonstrated and employed to measure electric fields around integrated circuit packaging connections.

External E-O probing is based on the use of an extremely small E-O crystal as a proximity electric field sensor near the surface of an integrated circuit as shown in Figure 1. This technique exploits the open electrode structure of two-dimensional circuits where there exists a fringing field above the surface of the circuit between metalization lines at different potentials. "Dipping" an E-O tip into a region of fringing field induces a birefringence change in the tip that can be measured from above by an optical beam directed through the tip. In this way, the E-O tip is employed as the modulator in a conventional E-O sampling system. By shining short pulses of light through the tip, synchronized with the electrical signal being measured, one can sample the electrical signal with a temporal resolution determined by the duration of the optical pulses.

It is because the E-O medium is separated from the integrated circuit that we call this technique *external* E-O sampling. By using an external E-O medium, the sampling system does not rely on any optical properties of the integrated circuit itself, hence making it generally applicable to a wide variety of circuit embodiments including silicon. This technique also allows for the use of E-O crystals that are transparent in the visible portion of the spectrum, thus enabling visible laser sources to be used.

As mentioned earlier, the option to relax speed requirements can be exploited in order to enhance sensitivity. A typical method of increasing sensitivity of conventional modulators is to increase the optical path length (given a fixed applied voltage). This ploy can be also be implemented in probe tip modulators by multiple passing the optical beam within the active region of the tip as shown in figure 2. By introducing a second high reflectance (HR) coating within the probe tip, an etalon can be produced which in effect traps a portion of beam in the active volume between the HR layers of the tip. This effect is analogous to intensity magnification within an optical cavity. If both HR mirrors have a reflectivity of 99% and a transmission,T, of 1%, the effective power level, or in our case sensitivity, increase between the HR's is equal to $1/T = 1/0.01 = 100$. This is equivalent to the number of passes through the fringing field region also increasing by the same factor. However, the increased sensitivity is achieved at the expense of temporal resolution, which is suffers by the factor of 100. But if the E-O tip thickness is in only 100μm, the temporal response will stillbe less than 1 ns and adequate for many applications in silicon testing.

What follows is an excerpt from our internal report on the F-P modulator together with some modelling data that was produced at a later date.

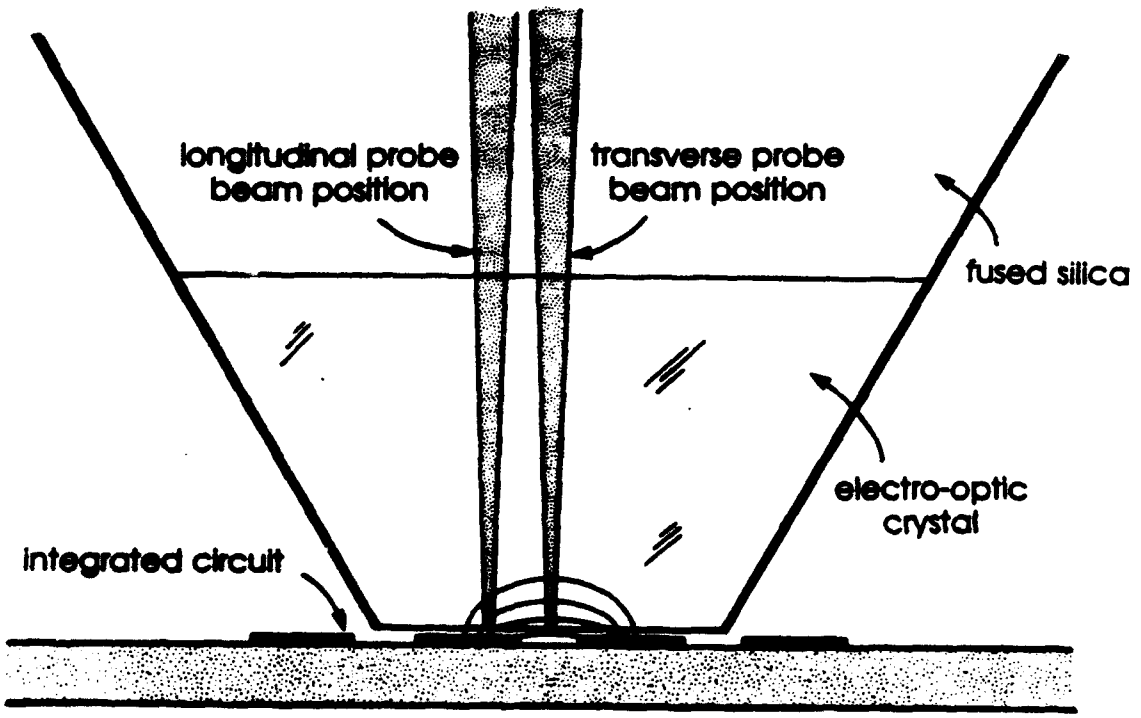

Fig. 1 Standard electro-optic probe tip

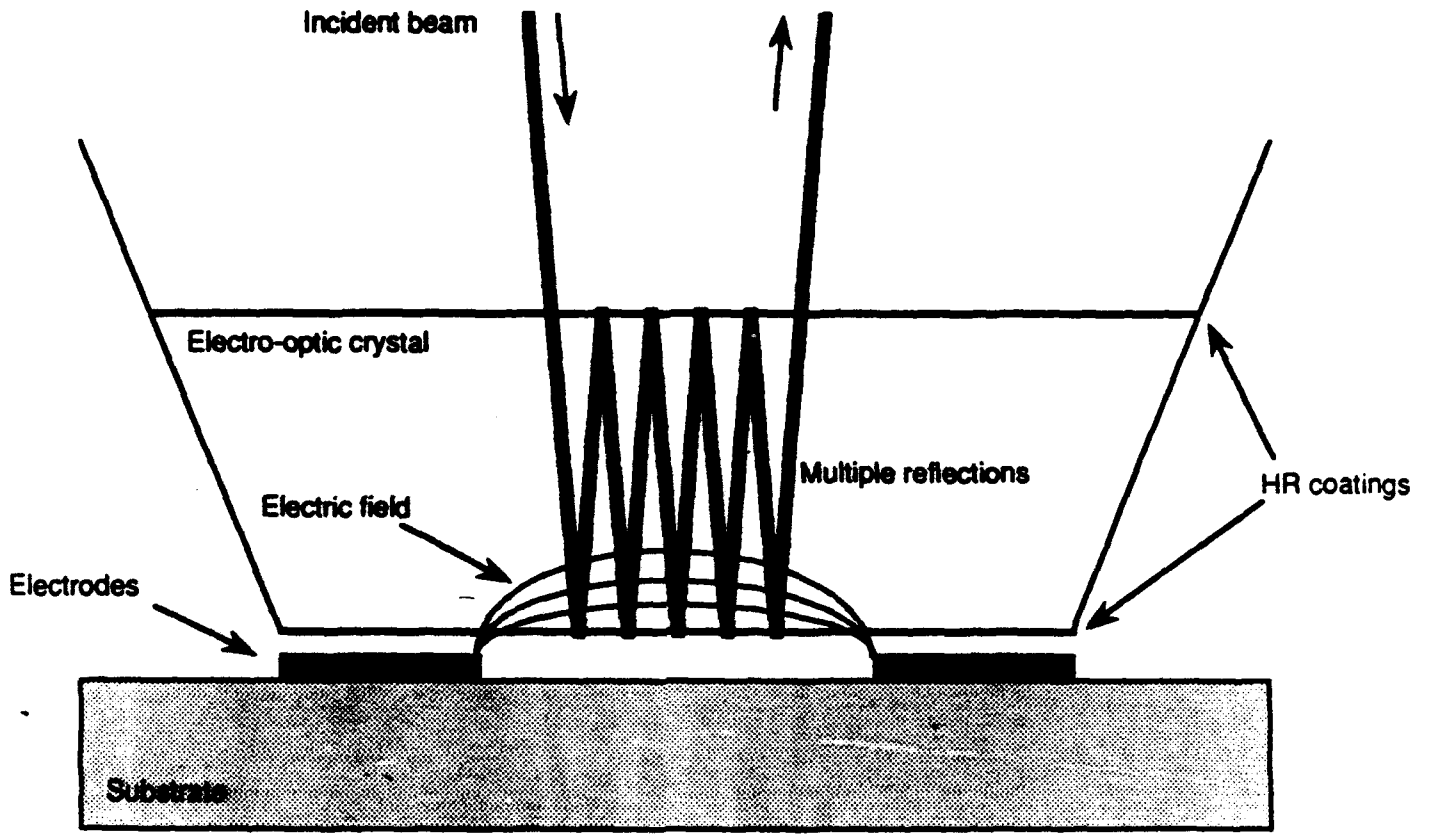

Fig. 2 Fabry-Perot electro-optic probe

Figure 3 shows the geometry of a Fabry-Perot electro-optic modulator. A second HR coating is added to electro-optic crystal, in this case lithium tantalate , in order to form the Fabry-Perot. The input beam is polarized in the z-direction in order to have maximum change in the index of refraction.

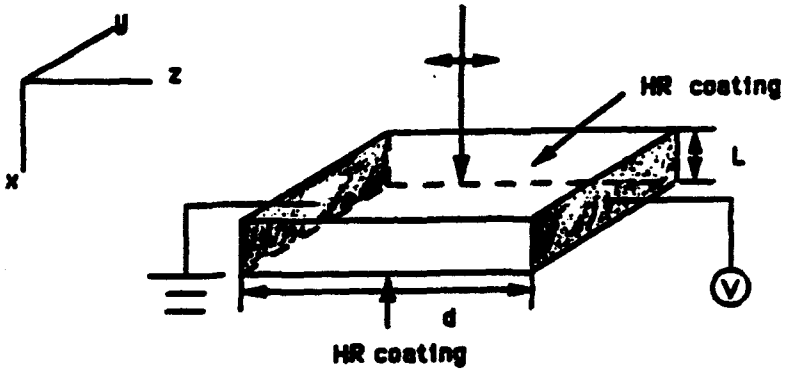

Figure 3. The geometry of a Fabry-Perot modulator

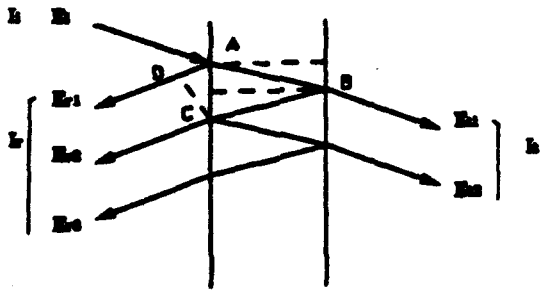

Figure 4.Multiple-beam interference within the Fabry-Perot etalon

By considering the multiple-beam interference problem as in figure 4, it can be shown that

$$\frac{I_r}{I_i} = \frac{4R \sin^2(\delta/2)}{(1-R)^2 + 4R \sin^2(\delta/2)} \quad (4)$$

$$\frac{I_t}{I_i} = \frac{(1-R)^2}{(1-R)^2 + 4R \sin^2(\delta/2)} \quad (5)$$

Where

$$\delta = \frac{4\pi}{\lambda_o} n_o L - \frac{2\pi}{\lambda_o} n_o^3 r_{33} \frac{V}{d} L \quad (6)$$

The δ corresponds to the optical pass difference, which is n[(AB)+(BC)]-(AD) in figure 4, between two successive rays. The corresponding plot of transmission is shown in figure 5 (R=85% on both surfaces of the crystal).

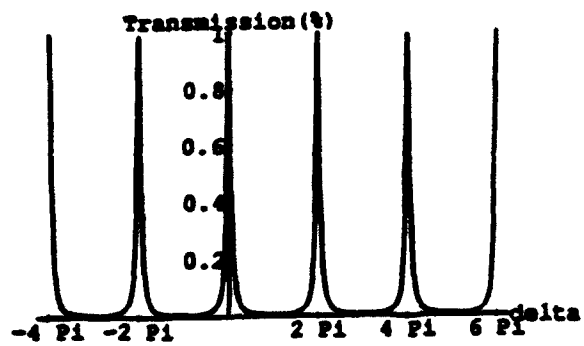

Figure 5, Transmission of Fabry-Perot etalon

As mentioned earlier, we used a compensator to bias the optical system so that the transmission is 50 % in the absence of the modulation voltage in the case of the normal modulator. For the Fabry-Perot modulator, however, the optical biasing or tuning method is different from the former case. There are a few ways of tuning in order to be at the point where the slope of

the transmission curve is the maximum which falls about 25% down from the peak value. One way of tuning is to tilt the crystal so that the effective crystal thickness changes. However, one should be careful about "walk off" effect of the beam because if the incident angle is too big, we will not able to get 100% overlap of successive reflections. Another way is to control the wavelength of the optical beam by using tunable diode laser. Other methods are applying bias voltage to the crystal and controlling of crystal temperature in order to induce a change in the index of refraction.

Some of the limiting parameters for this experiment are the linewidth of the optical source and frequency stability of the laser because, as shown in figure 8, modulation curve is a function of the frequency. Since finesse is very sensitive to parallelism of the crystal surfaces and quality of the crystal surfaces, these also can be limiting parameters. For example, with power reflectance of 85 %, the ideal value of finesse is about 20. However, finesse is degraded to 14.4 for surface imperfection of $\lambda/200$ and to 10 for surface imperfection of $\lambda/75$. The finesse of a Fabry-Perot etalon is the ratio of the separation of adjacent peaks to full-width half-maximum of a peak of the transmission curve.

In the ideal case, the sensitivity enhancement of a Fabry-Perot modulator over a normal modulator is expected to be about one half of the finesse of the Fabry-Perot etalon.

B. Experiment

The purpose of this experiment was to verify the expected result of sensitivity enhancement by measuring modulated output intensities of a normal electro-optic modulator and a Fabry-Perot electro-optic modulator

respectively when the equivalent voltage was applied. We have prepared coplanar electrodes with width of 200 micrometer on the microscope cover glass in order to simulate the internal node of silicon IC's. Although there are many crystals that exhibit electro-optic effect, we have chosen lithium tantalate crystal because it exhibits superior electro-optic coefficients relative to other materials. It is also environmentally stable and can be readily cleaned using common solvent. The Fabry-Perot etalon, was coated for power reflectance (R) of 85 % on both surfaces of the crystal. As mentioned previously, an optical source with a narrow linewidth and good frequency stability was desired because the transmission curve is a function of frequency of the source. Helium-neon (He-Ne) laser seemed very appropriate for the use because it offers the linewidth of about 1 GHz and frequency stability, $\Delta f/f$, of 1/1,000,000. The wavelength of the He-Ne laser was 632.8 nm.

First, we measured the finesse (F) of the Fabry-Perot etalon since it was essential parameter of determining the sensitivity enhancement. Because we used He-Ne laser,which was not tunable, as the optical source, we had to tilt the crystal in order to be at the point with the maximum slope of the modulation curve. The measured value of the finesse was 8.

The experimental setup of a Fabry-Perot type probe was as in figure 6.

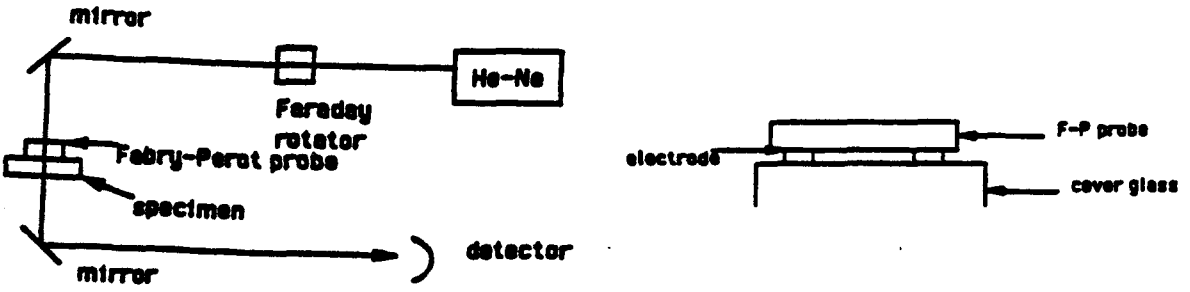

Figure 6.The experimental setup of a Fabry-Perot probe

The Faraday rotator was used to prevent the reflection directly back into the laser. The Fabry-Perot electro-optic probe was put on the specimen as shown in figure 6.

For actual measurement of modulation of transmitted beam intensity by voltage source, a sinusoidal signal of 14 V at 80 kHz of lock-in amplifier was applied to the electrodes and a sinusoidal waveform with 9 mV ac amplitude and 1 V dc offset was observed on the oscilloscope. (See Figure 15). Next, we used the setup shown in figure 7 in order to compare sensitivity enhancement of a Fabry-Perot electro-optic modulator over a conventional electro-optic modulator. The differences from the previous setup were additional polarizer, analyzer and compensator. With same input as previous experiment, 14 V, a sinusoidal waveform with 1.9 mV ac amplitude and 1V dc offset was observed on the oscilloscope. One should note that we used lithium tantalate crystal without HR coatings. Therefore, this was equivalent to half the sensitivity of the case using HR coating with R=1 on the bottom surface as in a conventional electro-optic modulator.

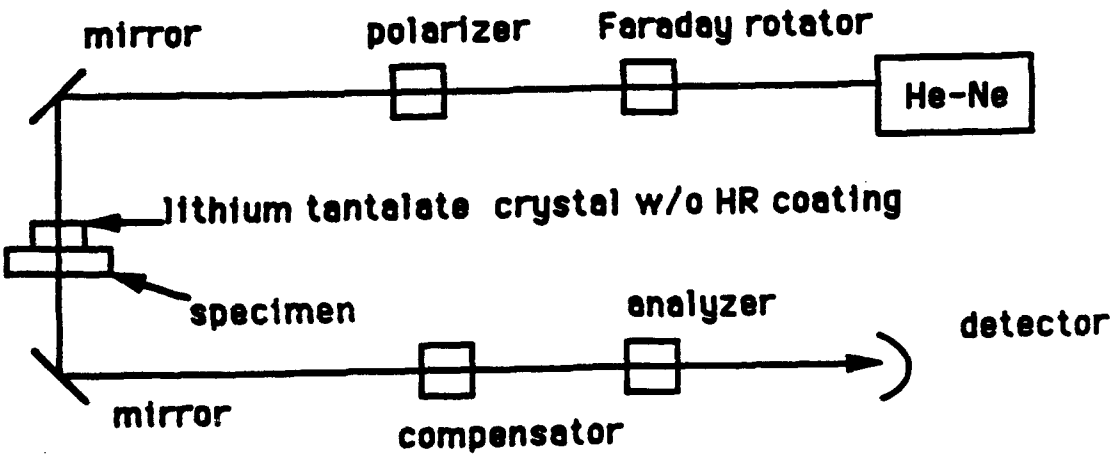

Figure 7 The experimental setup for normal probe

This corresponded to little more than twice the sensitivity enhancement of a conventional electro-optic probe by using a Fabry-Perot etalon with F=8.

C. Analysis of Experimental Results

Analyzing the data of experiment, we found that the finesse of the crystal was lower than the theoretical value. The target was finesse (F) of 20 by 85 % of high reflectance (HR) coating on both surfaces of the crystal. But experimental value was F =8. The discrepancy between the theoretical value and the experimental value of the finesse had to be from one or more of following reasons;

1. Loss due to the scattering
2. Reflectance mismatch between two surfaces
3. Surface imperfectness and/or parallelism

By measuring transmitted beam intensity, reflected beam intensity and input beam intensity, we could measure the scattering loss assuming the absorption in the crystal was negligible. The experimental value of scattering loss was about 15 % of the input beam.

We also measured reflectance of the crystal by measuring the maximum and minimum transmitted intensities of the crystal and compared it with calculated transmission curve due to the "etalon effect". We found out that HR coating on two surfaces of the crystal did not match closely. The difference between two HR coating was more than 10 %. Figure 8 shows the transmission curve with different R values on the surfaces of the crystal.

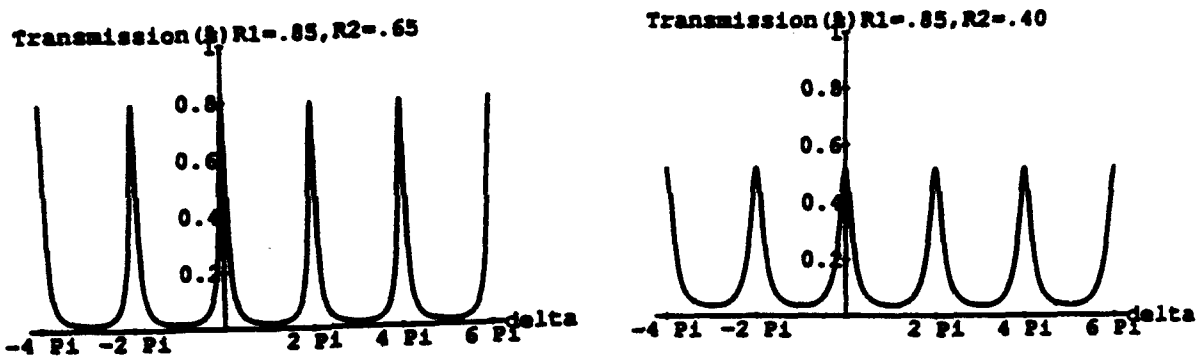

Figure 8 Transmission curves due to the "etalon effect"

Next, we checked the parallelism of the crystal. Although it was hard to get the exact quantitative value of the deviation from the perfect parallel surfaces, we found it was approximately $\lambda/100$ or less over the beam spot size (about 1mm) because lithium tantalate wafer was polished to $\lambda/8$ over 1 inch in diameter.

The difference of experimental value (2.4) for sensitivity enhancement and calculated value (4) was due to following reasons. First of all, finesse of the crystal on the cover glass with electrodes (F=7) was lower than its value of crystal alone(F=8) because the Fabry-Perot etalon-cover glass interface and glass-air interface were formed instead of the Fabry-Perot etalon-air interface. Secondly, when transmission peaks are decreased and width is broadened due to reflectance mismatch as indicated in figure 8 , the sensitivity enhancement is less than the ideal case, $F/2$ because the point with maximum slope of modulation curve is also shifted.

Figure 9 shows the sensitivity enhancement one should expect as a function of the power reflectance of the coatings on the lithium tantalate crystal. All our work was done in the range of 85% R in order to get approximately a factor of 10 enhancement. Most of the experimental work was done in reflection from the modulator, so that in figure 10a the intensity at resonance decreases. Fig's 10a and 10b show the effects of mismatched reflectances from the two sides of the crystal. One side is held at R=90% while the other is varied. It is clear that the sensitivity enhancement critically depends on having a good R match. This was found to be part of the problem experimentally. Fig. 11 shows the sensitivity enhancement normalized to that of a normal LT probe without F-P coatings. The peak value occurs at the point of steepest slope in the intensity function and is over a factor of 10 for R=92% coatings.

In order to tune the F-P to the peak sensitivity, one could either tilt it or tune the wavelength of the laser. Fig. 12 shows the effect of tilting to move over the transmission peaks. A few degrees is sufficient, but the drawback is that the beam can walk-off itself by more than a spot size also, so this is not a preferred method. Fig. 13 shows that the same can be accomplished by tuning the laser by only a fraction of a nanometer. We demonstrated this effect by using a diode laser around 800 nm as shown in Fig. 14. As can be seen, a change in wavelength of only 0.005 nm changes the sensitivity by a factor of 2. Figure 15 shows the real time experimental results we obtained with a 10 volt rms applied signal at acoustic frequencies. These results verified our calculations of increased sensitivity over a regular e-o probe. We also could see the effects of focussing the optical beam into the modulator. The larger range of angles in a focussed beam decreased the overall sensitivity, thus indicating another trade-off involved between spatial resolution and sensitivity.

In conclusion, this work has demonstrated the principles of F-P enhancement, but also reminded us of the fact that good, bulk F-P's are very hard to make. It seems highly unlikely that an adequate finesse could be achieved to increase the real time sensitivity to acceptable levels, even though speed of response would be easily met. This will probably rule them out as an option for this application regardless of the spatial resolution issue.

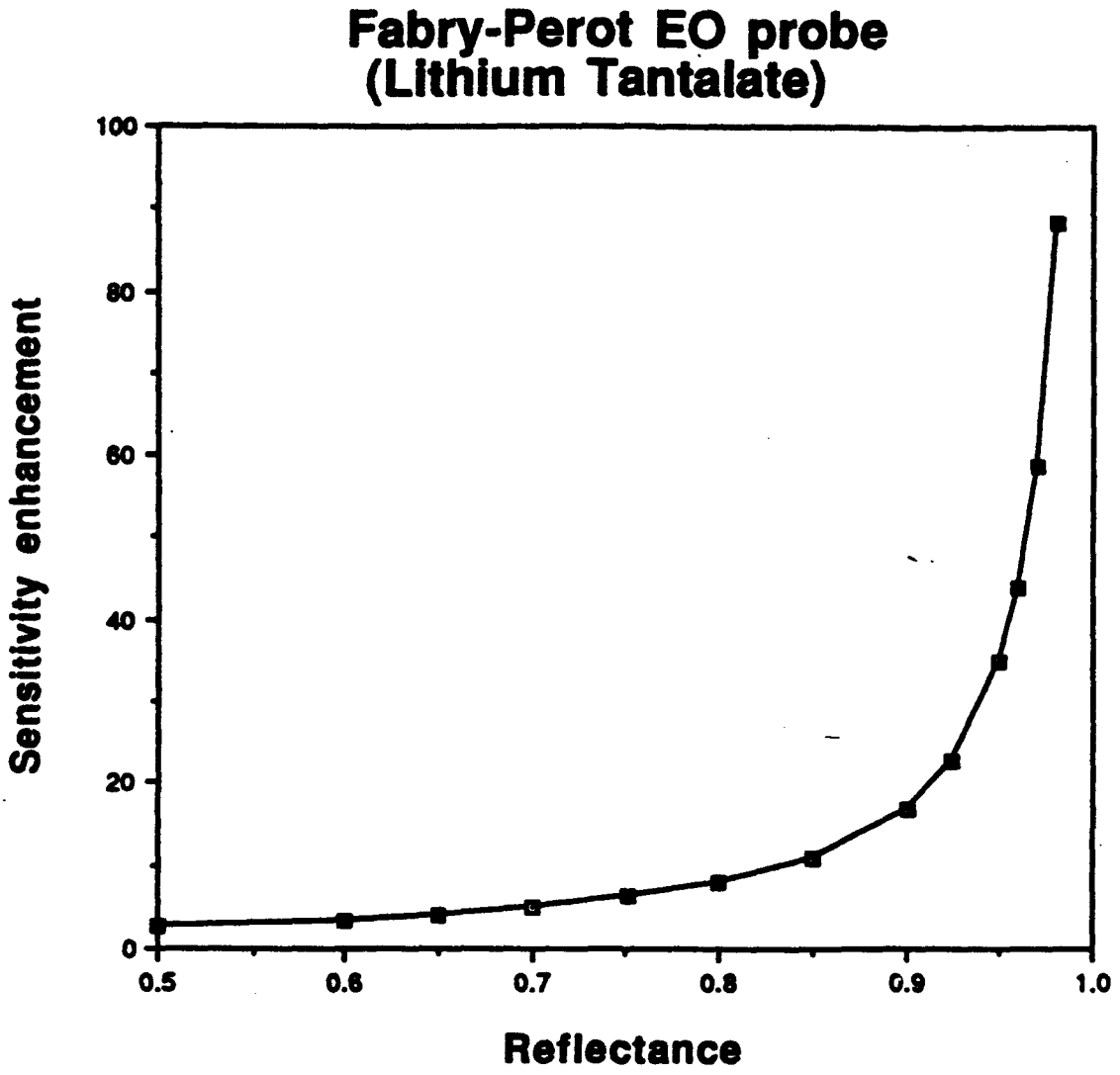

Fig. 9 Fabry-Perot sensitivity enhancement

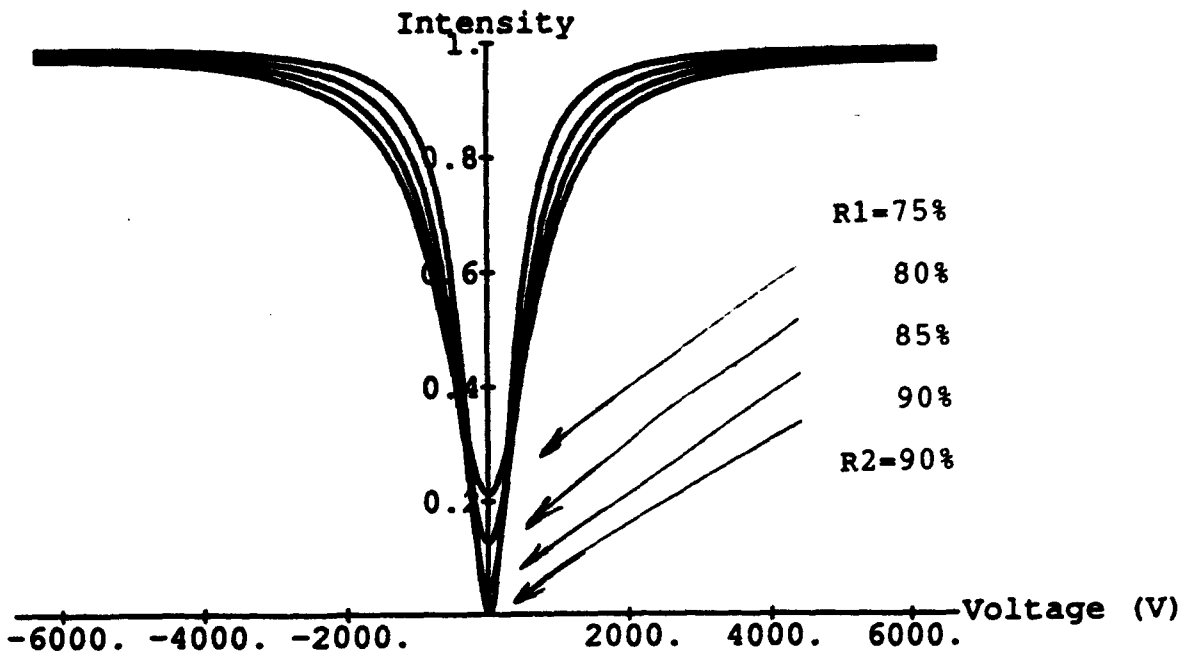

Figure 10a. Effect of mismatched F-P reflectances on Intensity.

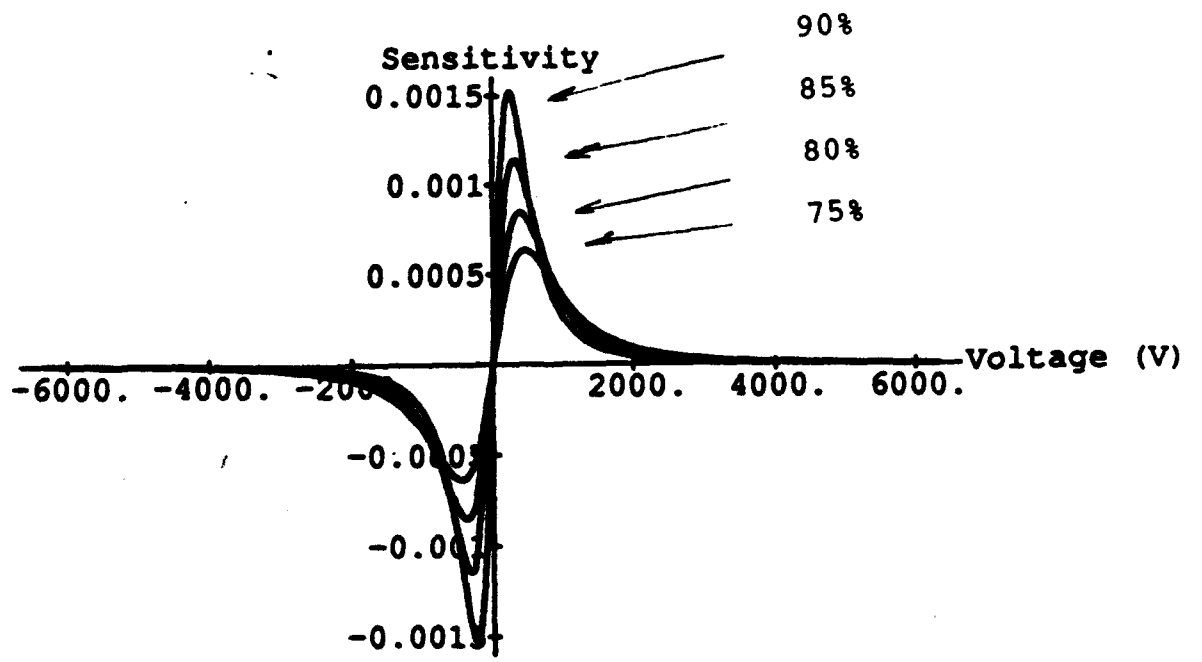

Figure 10b. Effect of mismatched F-P reflectances on Sensitivity.

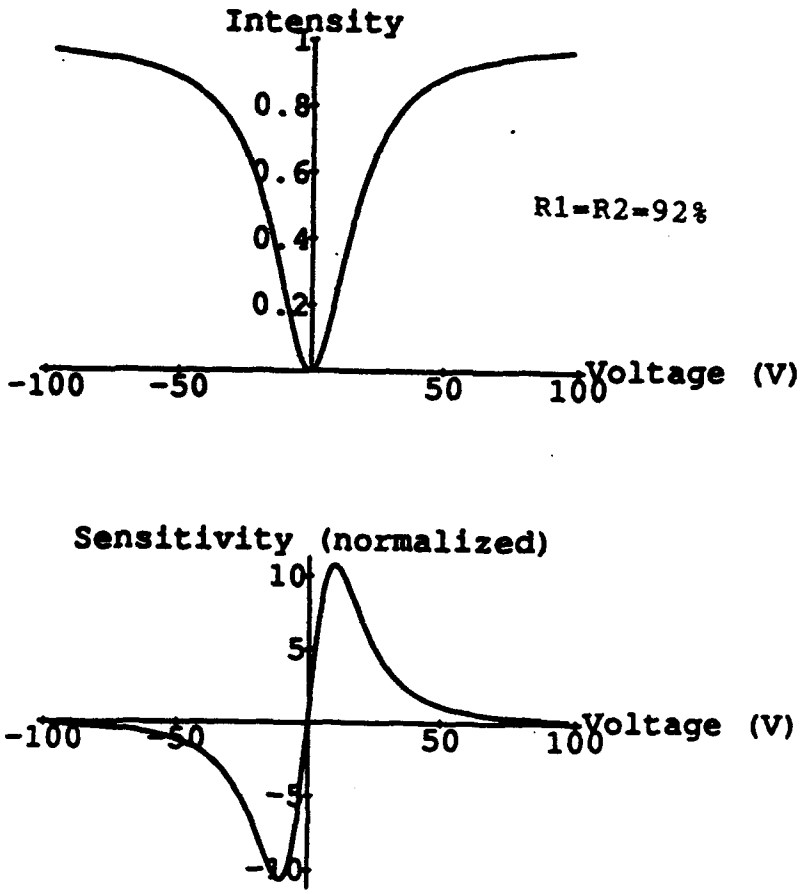

Fig. 11 Sensitivity enhancement

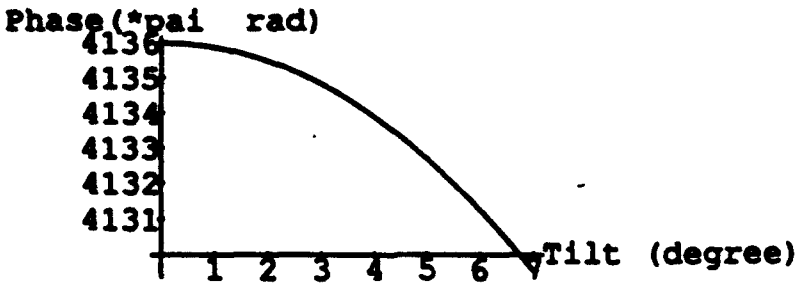

R1=R2=92%

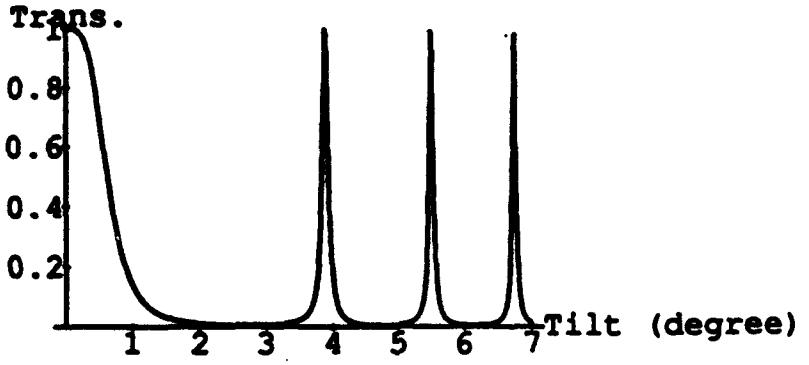

Walk off(thick.=300.05 um)/round trip

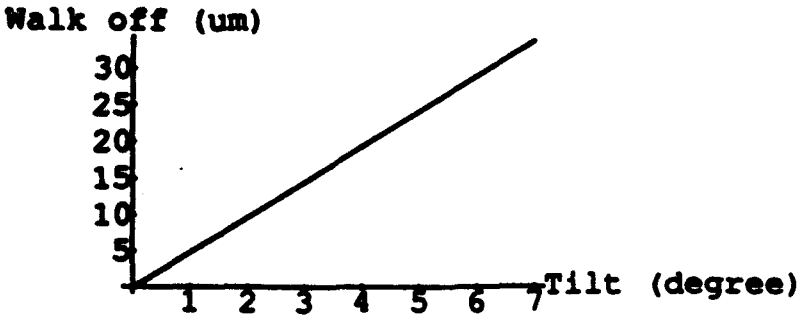

Fig. 12 Effect of tilting Fabry-Perot

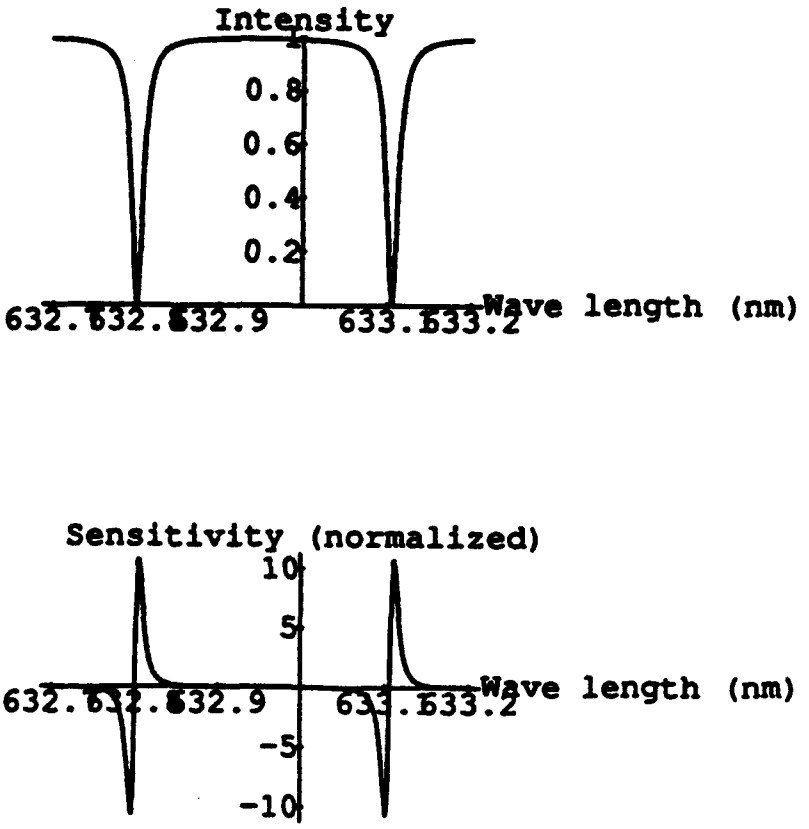

Fig. 13 Effect of laser tuning

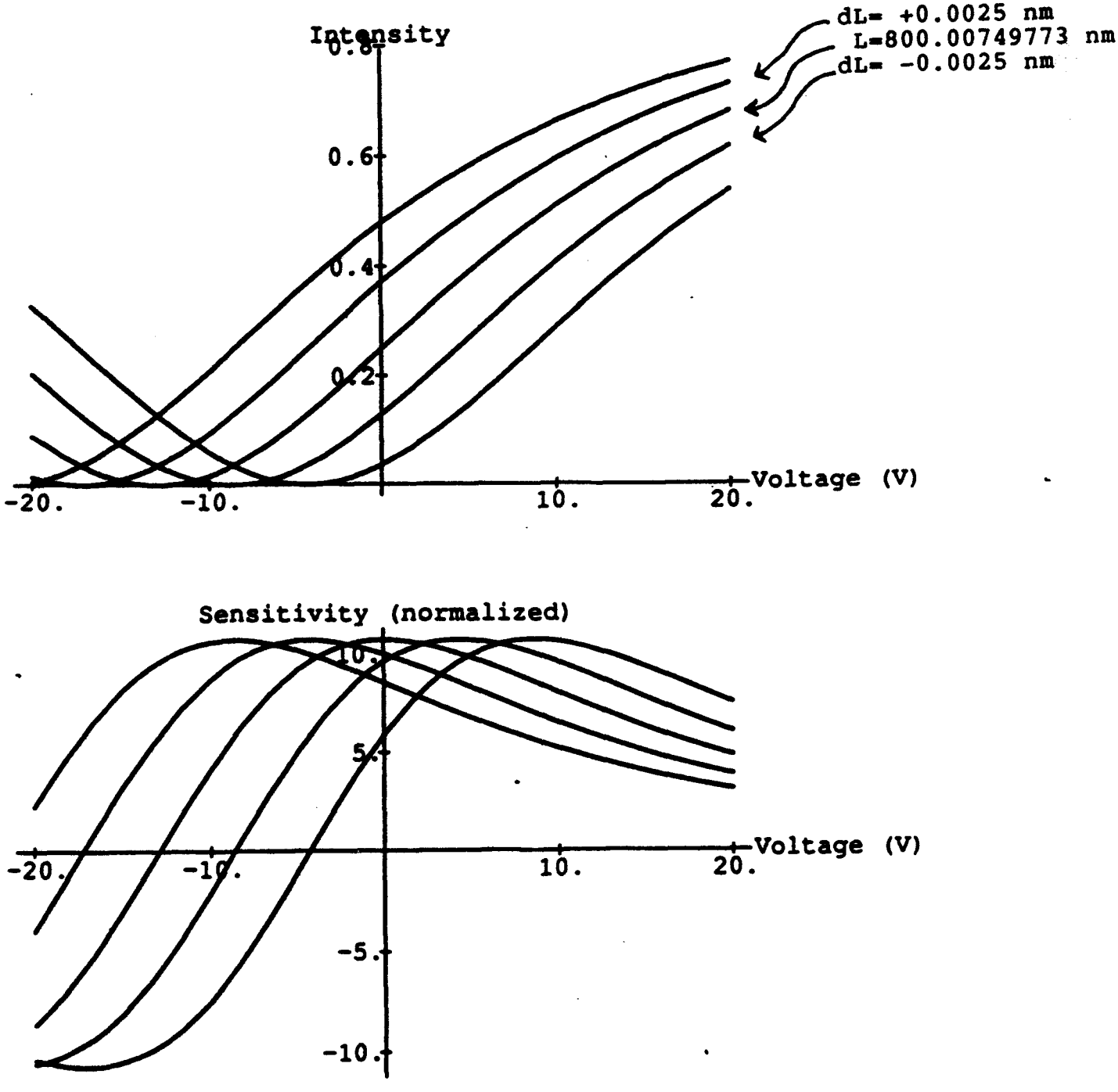

Fig. 14 Effect of laser tuning

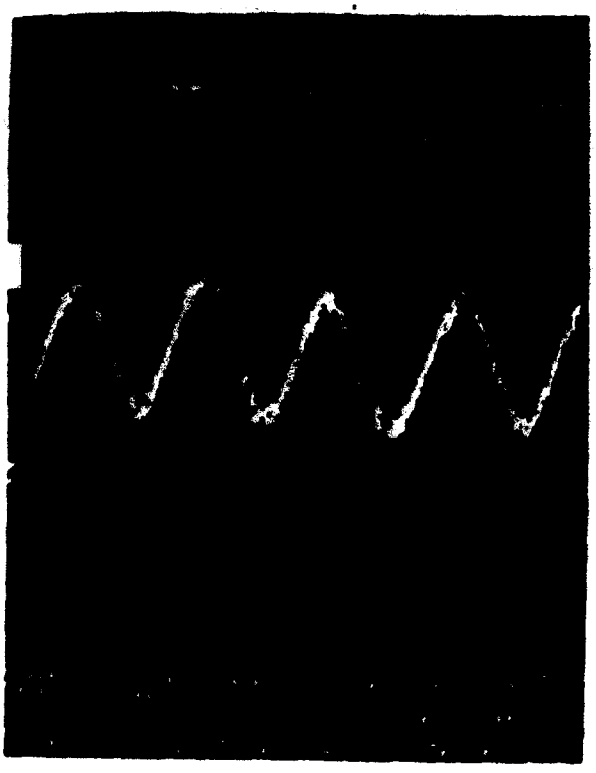

[with focusing lens (f=50mm]

AC=6mv (amp.)
DC=+1.2v

Ref.
DCmax=+1.93v with crystal
DCmin=+0.15v and specimen

DC=5.4v with specimen
DC=6.2v with nothing

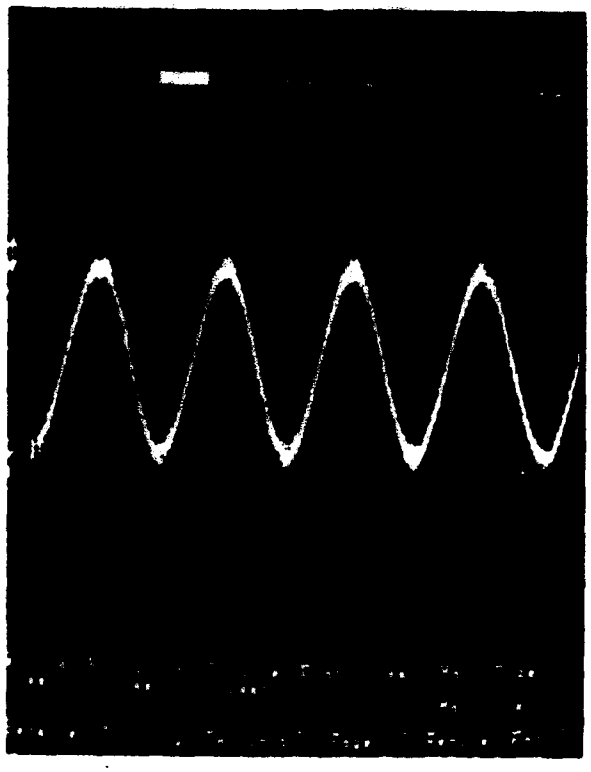

[without focusing lens]

AC=6mv (amp.)
DC=+1.0 v

Ref.
DCmax=+1.75v with crystal
DCmin=+0.14v and specimen

DC=3.15v with specimen
DC=7.2v with nothing

Specimen = 200um line electrode & space

Input signal = 2 x 10v (amp). by Lock-in Amp. VCO.

Figure 15. Experimental Results using F-P modulator.

III. MQW electro-absorption modulators

A. Introduction

A new class of materials has been emerging over the past years that holds great promise for field sensitive optical modulation, i.e. MBE grown, engineered semiconductors. Using MBE, multiple quantum well structures have been grown that exhibit what is known as the quantum confined Stark effect (QCSE). In these structures it has been shown that electric fields applied to the quantum well structure shift the absorption edge to lower photon energies thus increasing the absorption of light with a photon energy near the edge. By forming a structure of this type into a probe tip, and transmitting light of the appropriate energy through it, it would be possible to employ this effect as the external modulator. This is attractive because in some material structures, the QCSE has been shown to be significantly more efficient than the E-O effect.

This work was done in collaboration with Ran-Hong Yan, formerly at UCSB, but now at AT&T Bell Labs at Holmdel, NJ. He very generously supplied us with modulator samples and advice on their implementation. Yan's work has resulted in the most efficient modulator of this type ever produced [2], and we were able to test its applicability to IC probing.

B. DC testing

The transducer is a MQW asymmetric electro-absorbtion (e-a) type Fabry-Perot structure as shown in Fig. 1. The active layer is sandwiched between two mirror stacks that are grown along with the MQW layer itself. In this way, the active layer is less about 0.5 μm thick, and the doped mirrors act as the conducting electrodes producing an extremely high field across the active layer. This type of modulator has achieved a modulation efficiency of up to 23% per volt which is hundreds of times larger than that for the straight lithium tantalate E-O modulator. The drawback is that if the field is to be applied directly to the active layer, then one of the mirrors must be in contact with the circuit electrode to be measured. This is the mode that we have investigated.

Initial experiments were designed to characterize the properties of the samples we had obtained. Fig. 2 shows the set-up used to evaluate the spectral response of the sample. This was done with a monochrometer, and the resultant spectrum is shown in Fig. 3. Here you can see several of the standard features of these types of devices, i.e. the MQW exciton peaks and the F-P peaks. With the application of a reverse voltage, the MQW peaks shift to the red as they are supposed to do. The separation between the MQW peak and the F-P peak is approximately 8 or 9 nm, and the maximum reflectance is about 95%. The bandwidth of the F-P peak is also important so that extremely narrow band lasers need not be used. These samples give more than 10%/Volt modulation over a bandwidth in excess of 5 nm. The region of highest sensitivity is around 860

nm. This can be seen by comparing the reflected power for the case with no voltage applied to that with -1.5 V applied. This agrees also with Yan's results, and is precisely the wavelength that we will operate at in this application.

Fig. 4 shows the arrangement used for making electrical measurements to the samples at the same time as the optical measurements. The bottom metalization was attached to a finger that held the sample and then the top contact was made by a standard needle probe. This set-up was not designed to investigate any speed issues. The I-V curves were checked with and without illumination to see that the devices operated with the proper diode type behavior as shown in Fig. 5.

The slow speed modulation behavior was also checked at this stage by the set up shown in Fig. 6, where a cw Ti:Sapphire laser was used as the light source. The center wavelength was chosen to be 860 nm, with about 1 mW of power going to the sample. A typical modulation result is shown in Fig. 7 where a DC offset voltage of -1.5 V was applied together with a sinusoidal drive voltage of +1 to -1 V. The resultant curve is highly nonlinear due to the nonlinearity of the response curve. This will have an effect in limiting the dynamic range of this probe, although this parameter could be tailored to suit various needs. The nonlinearity changes form as a function of wavelength because the shape of the spectral response varies also.

These samples also show the presense of a large photocurrent in response to illumination which could present a serious problem in the probing application, because it would affect the signals in the circuit. This feature is demonstrated in Fig. 8. Although this is a problem in these electro-*absorption* type modulators, it is not so in electro-*refractive* modulators of the same type. In that case, the absorption in the active layer is negligible and no photocurrent is generated. The basic F-P principles in both types of modulator is the same, so other features that we have studied will apply to the non-absorbing types also.

C. Sensitivity

Figure 9 shows the experimental arrangement used for testing the MQW modulators as high-speed probes. A more detailed top view of the sample structure is shown in Fig. 10. The MQW modulator is mounted on the end of a metallized glass arm so that its bottom electrode can be used as probing contact. This arrangement is designed to imitate a real probing situation, but without the high spatial resolution requirement. The top contact is wire bonded to a pattern line that leads to the outside world. The entire setup is mounted so that the laser beam has free access to top surface of the modulator, while the modulator sample electrodes can be electrically to any outside source like DC power supplies, curve tracers, frequency synthesizers, or the tested electrode.

As shown in the series of I-V curve data as a function of wavelength in Fig. 11, the highest sensitivity to modulation is near 862 nm for this sample. The corresponding real time modulation curve is shown in Fig. 12, where the upper trace is the input voltage, and the lower trace is the modulated beam power. It can be seen there are linear regimes where this particular modulator in fact could be used reasonably. The linearity of response can be adjusted by applying a suitable offset voltage to the sample as is shown in the following figures taken at the peak response wavelength of 862.4 nm. Fig. 13 shows the response to modulation with no offset voltage; it is highly nonlinear. With -1.75 V offset, as in Fig. 14, we get a fairly symmetric response function over an applied voltage range of ±1 V.

We also measured the minimum detectable real time signal using this particular modulator. Fig. 15 shows the result of averaging 16 real time scans with 25 mV applied to the electrode being probed. It can be seen that the minimum detectable signal is around 5 mV. Without averaging the min. signal is about 20 mV. This meets the requirement originally specified in the work statement of ≤ 50 mV. Incident laser power was about 0.3 mW, and the detector load resistance was about 5 kΩ. There are many contributions to the noise, but in this case our laser was the dominant source. A quieter laser source, e.g. laser diode, would increase sensitivity significantly.

D. Temporal response

In these tests, a high frequency signal was applied to the test lines to see what the maximum speed capability of the modulator would be. A high speed detector system was used to monitor the modulated beam. The signal was of 1V amplitude with an offset of 1.9 V to get maximum resonse. Initial tests indicated a bandwidth of only about 12 MHz, before significant response rolloff occured. By grounding the top electrode instead of letting it float, we wee able to extend the bandwidth to about 16 MHz. Since this was clearly not acceptable, significant changes were made in the design of the probe support and electrode structures, as well as the associated cabling. The new probe is shown in Fig. 16. In addition, a new, smaller, chip modulator was used, and the polarity of the signal was reversed so that the bottom electrode was grounded and the top one carried the high speed signal. In this case, the bandwidth only increased to about 20 MHz. Without the opposite electrode grounded, the bandwidth was still 12 MHz, as before. This performance was very poor, and we started to take a closer look at what could be contributing to the problem.

It turns out these devices seen in Fig. 17 were only designed for DC operation; i.e. no care was taken in the design to worry about any speed limiting parameters. Capacitance across the active area is difficult to do anything about. One can only reduce the area of the active portion to reduce the capacitance, but this in turn raises the series resistance of the device. We discovered

that the real problem was that even though the MBE grown electrodes were doped to be conducting, the abrupt junctions to the MQW layer were creating a very high series resistance. This very simply increases the RC time constant of the device. Fig. 18 shows the circuit model that was considered in this study. Junction capacitance is calculated to be roughly 70 pF for a 0.8 mm x 0.4 mm x 0.5 μm active volume with ε of 13. Series resistance is calculated to range from 2 kΩ to several hundreds of kΩ for the abrupt interfaces, which puts the bandwidth in the MHz range as we have found experimentally. Issues concerning the transit time of the laser beam and of the photo-generated carriers were also considered, but are not of the magnitude we are worried about as pertains to speed.

R-H Yan was able to suuply us with new devices that had less series resistance in the mirrors. These were also fabricated as mesa structures in order to reduce capacitance. In these devices R= 200kΩ for a 10mm diameter dot, so that R_s is estimated to be about 50Ω for a 0.32 mm^2 device. This means RC should be about 3.6 ns and the corresponding bandwidth about 100 MHz which once again would satisfy the work statement requirement for speed.

If the carrier lifetime were too long, the internal field may be reduced due to space charge effects. This would depend on the incident power level. The recombination time in these types of MQW's is on the order of nanoseconds, but if the power level is kept below roughly 1 mW into a spot 10μm in diameter, then a 1 GHz bandwidth should be attainable. Drift times in these devices should be on the order of about 15 ps.

Figure 19 shows the geometry and experimental arrangement used for testing the mesa structures. In these samples the optimum wavelength was about 857-860 nm. A sinusoidal signal of 500 mV amplitude was applied to the probed electrode. DC offset was supplied to get maximum modulation. The frequency was swept to check maximum response up to a detector system limit of 350 MHz. Incident power level was set at 0.8 mW, and the offset level was -5.9 V. As shown in Fig. 20, this modulator easily exceeded 100 MHz and in fact had a 3dB down point of about 190 MHz. For this particular device, the junction capacitance was estimated to be about 3 pF and the series resistance about ≤ 20 Ω. Other factors contributing to the loss of speed are probably source resistance (≈50 Ω), contact resistance, electrode resistance, and other stray capacitances and inductances. Without these, 1 GHz should be attainable.

E. Conclusion

Summarizing the findings of this study of using MQW modulators as circuit probe transducers for this work statement we find:

- Speed of response is adequate, almost 200 MHz

- Sensitivity is adequate, less than 20 mV real time
- Photo-generated current is probably too large to be non-invasive
- Present devices are too non-linear over needed range of few volts

A possible solution to the two latter problems is the use of electro-refractive modulators instead of electro-absorptive modulators. These do not have the photo-current problem because they do not absorb any light, but they are also less sensitive to applied voltages by about a factor of ten currently. However, the decrease in sensitivity can actually buy an increased dynamic range if the laser noise can be reduced. This is not out of the question and could be pursued.

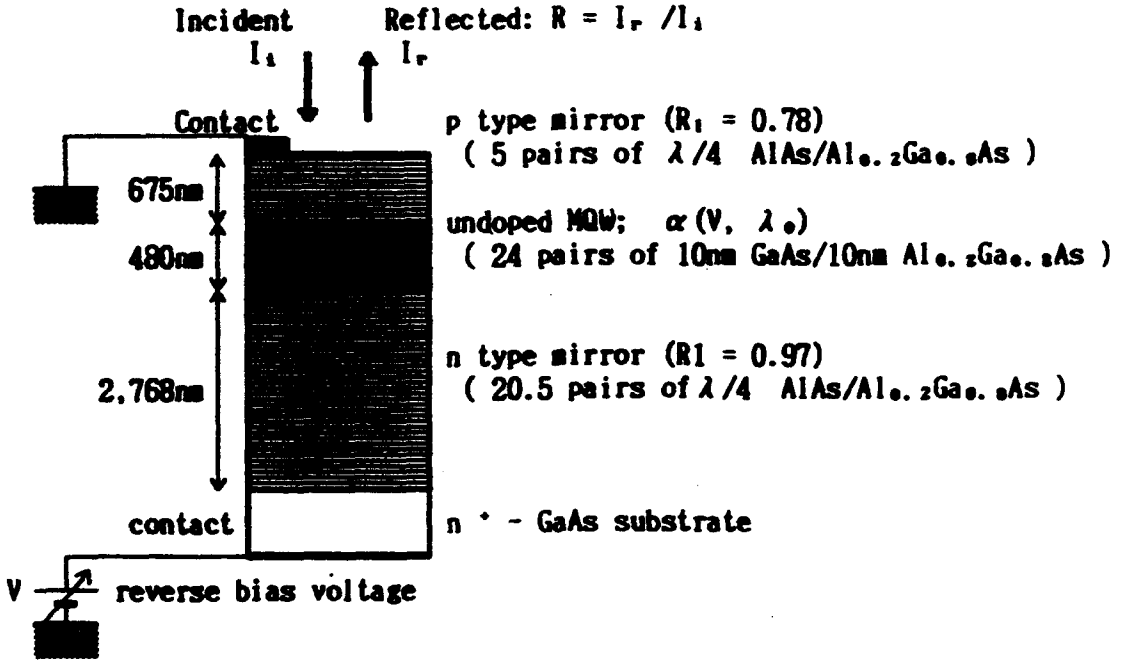

Fig. 1 MQW electro-absorption modulator

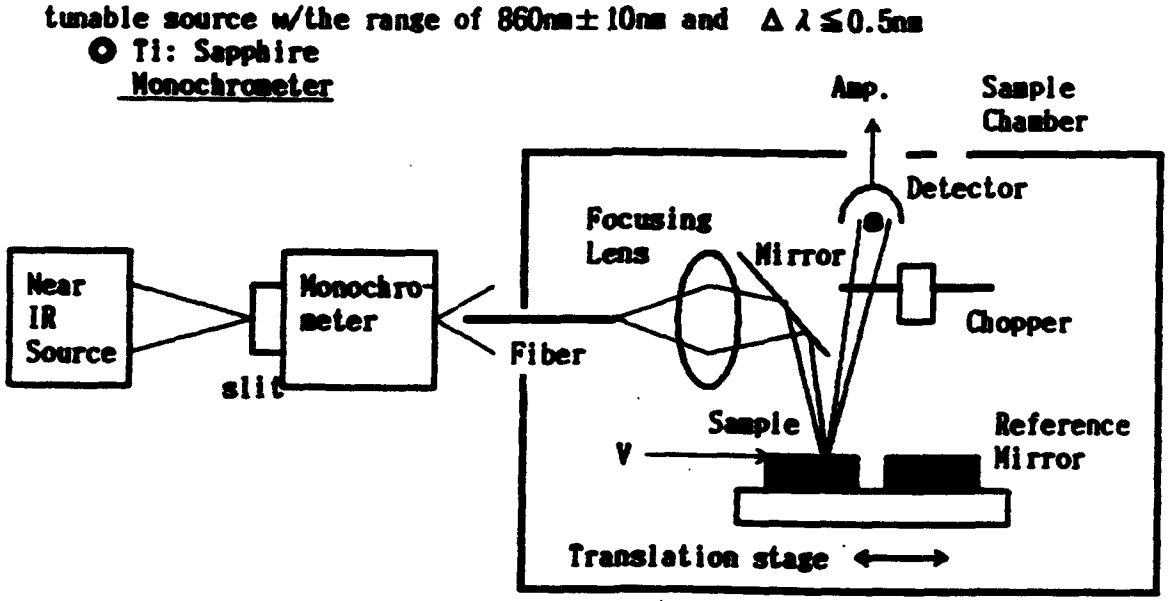

Fig. 2 Spectral testing set-up

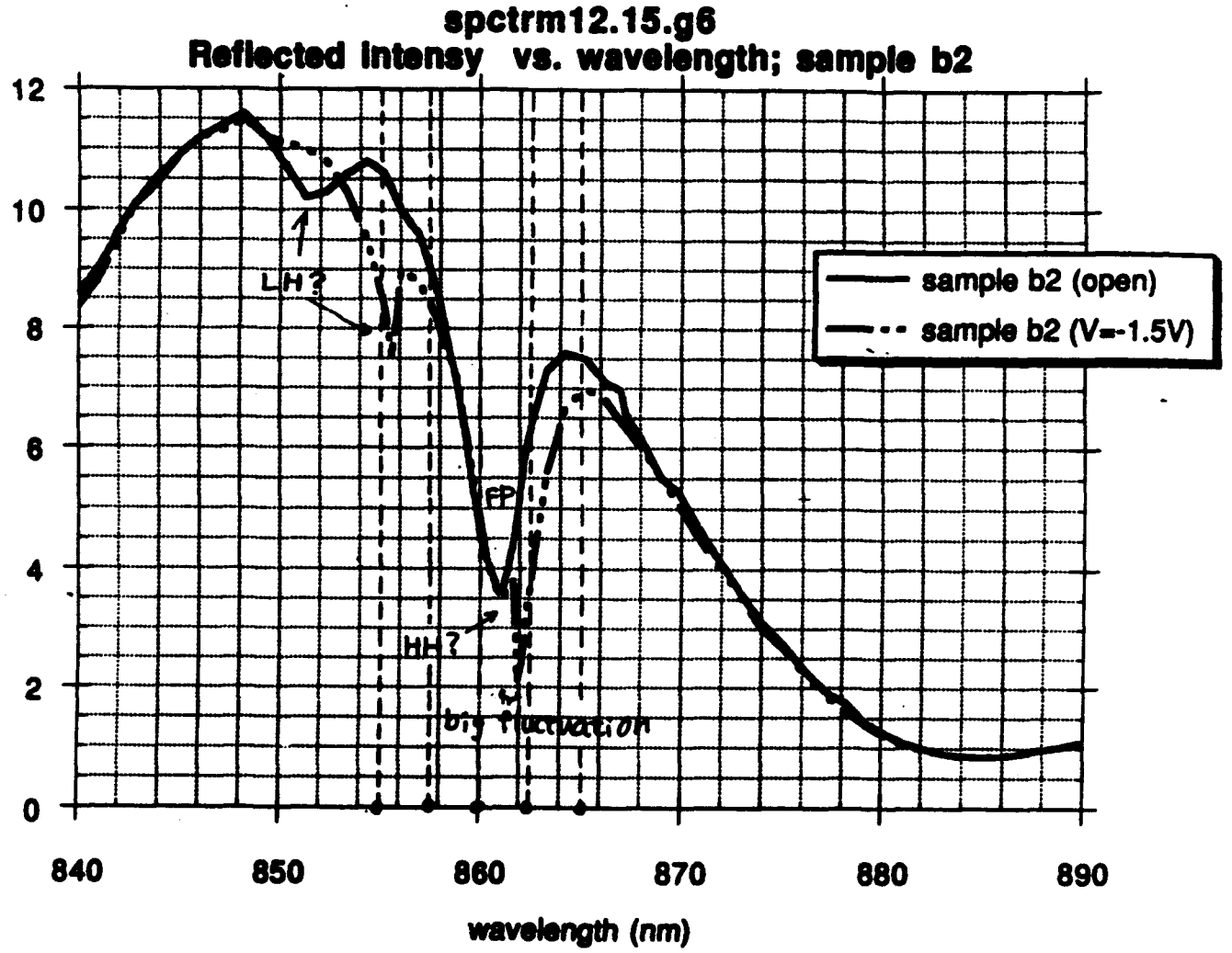

Fig. 3 MQW modulator spectral response

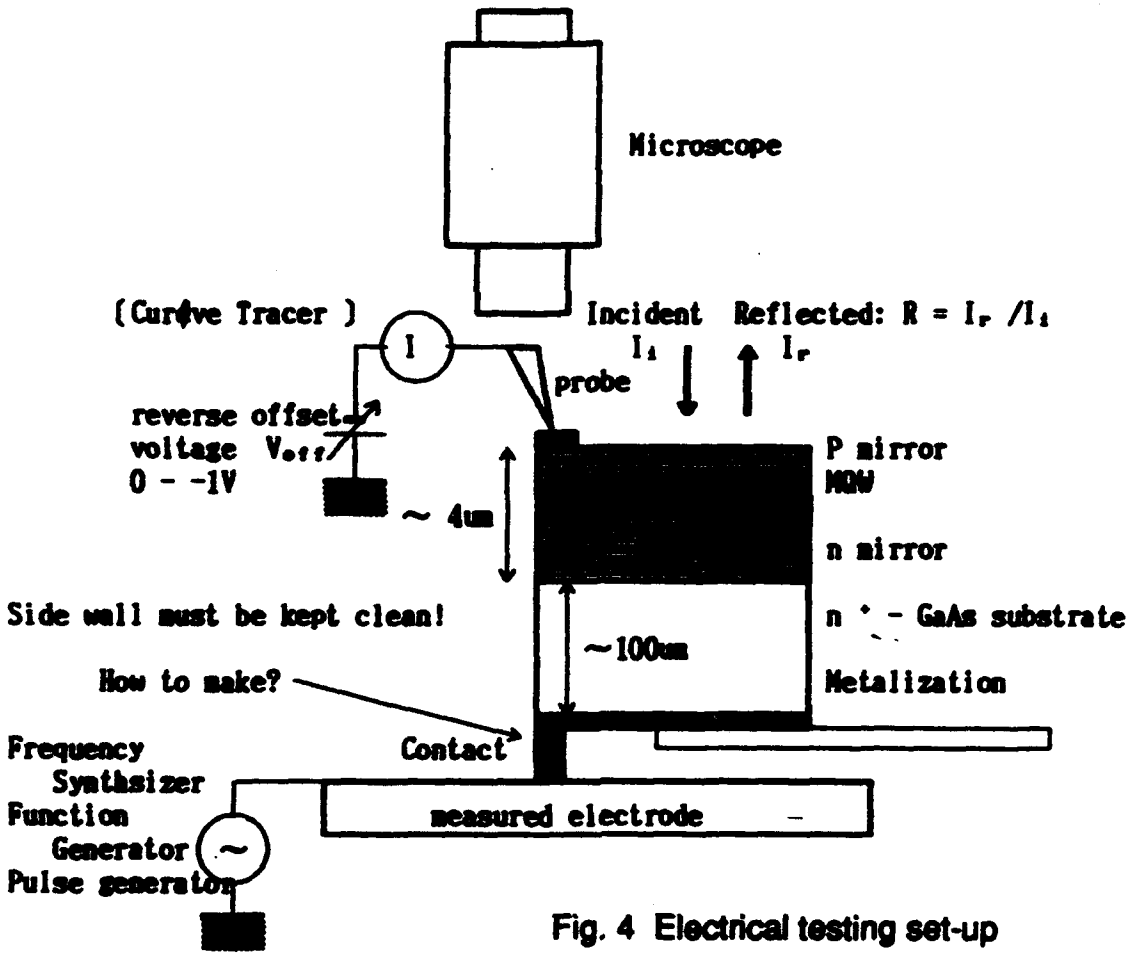

Fig. 4 Electrical testing set-up

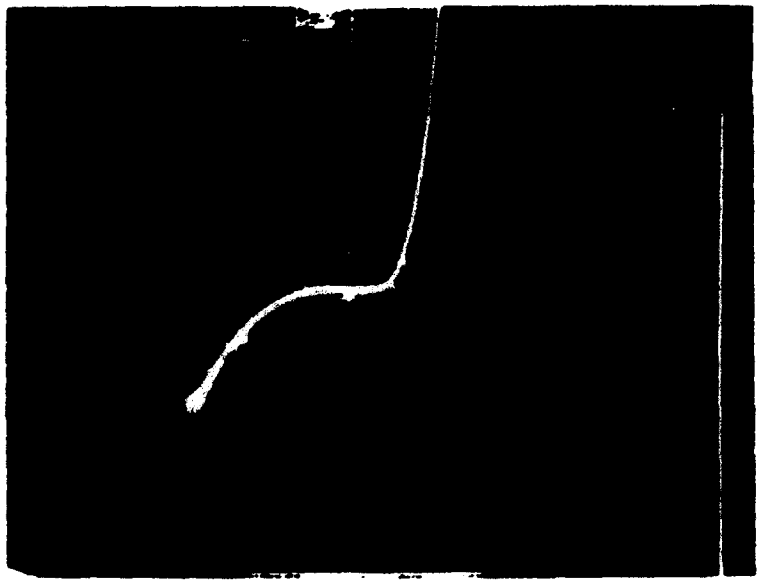

Fig. 5 I-V behavior

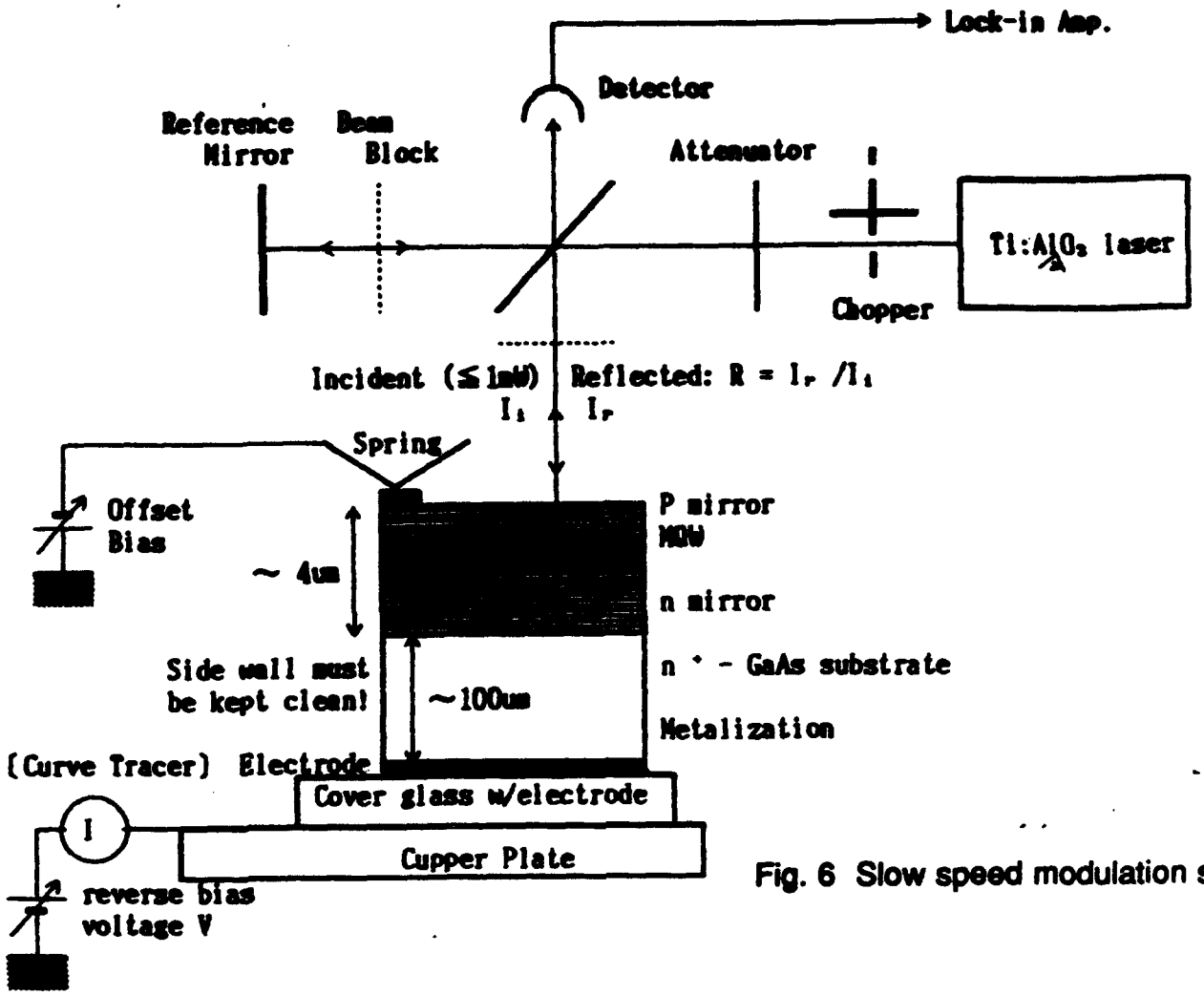

Fig. 6 Slow speed modulation set-up

Figure 7. Slow speed modulator response.
(L=364-859.5nm Offset bias=-1.5v)

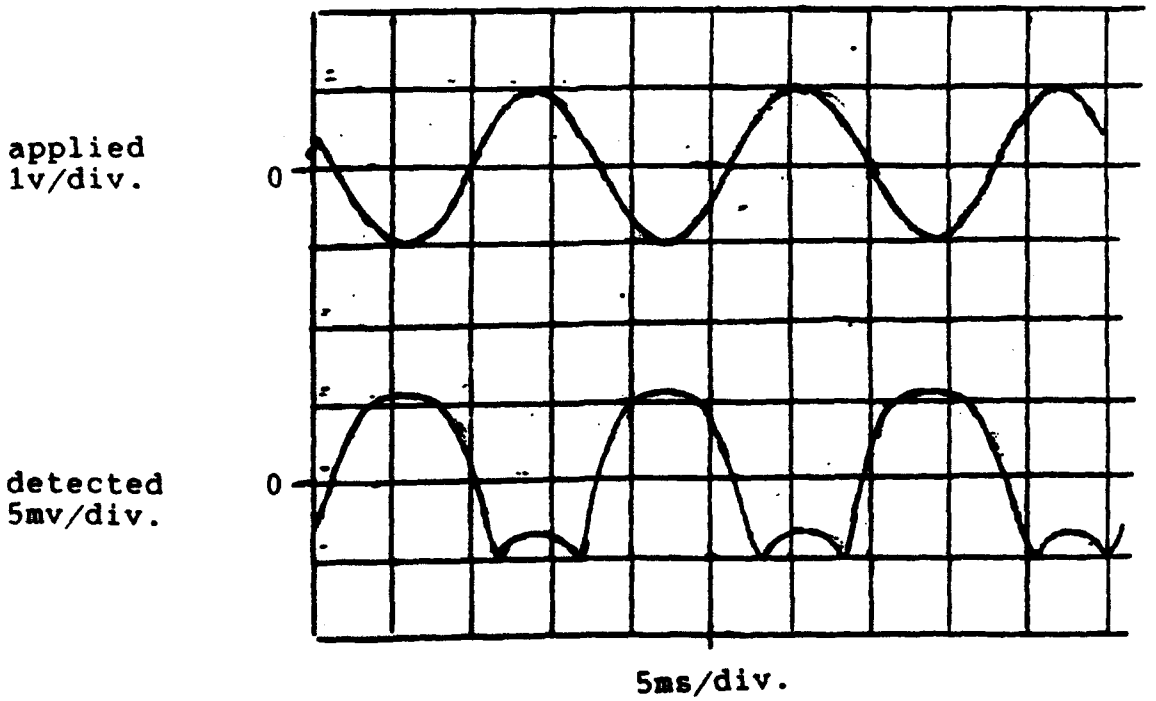

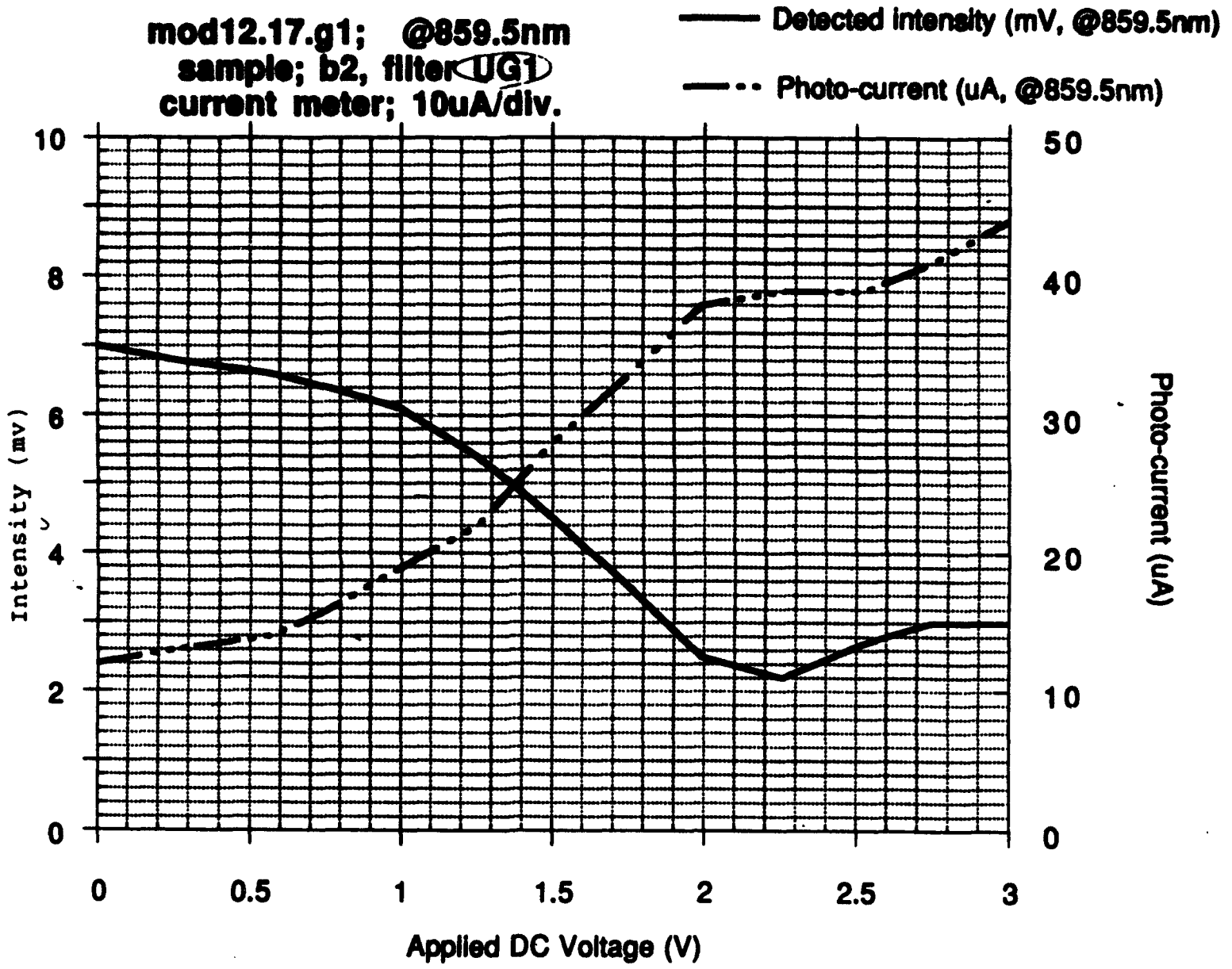

Fig. 8 Effect of photocurrent on modulator response

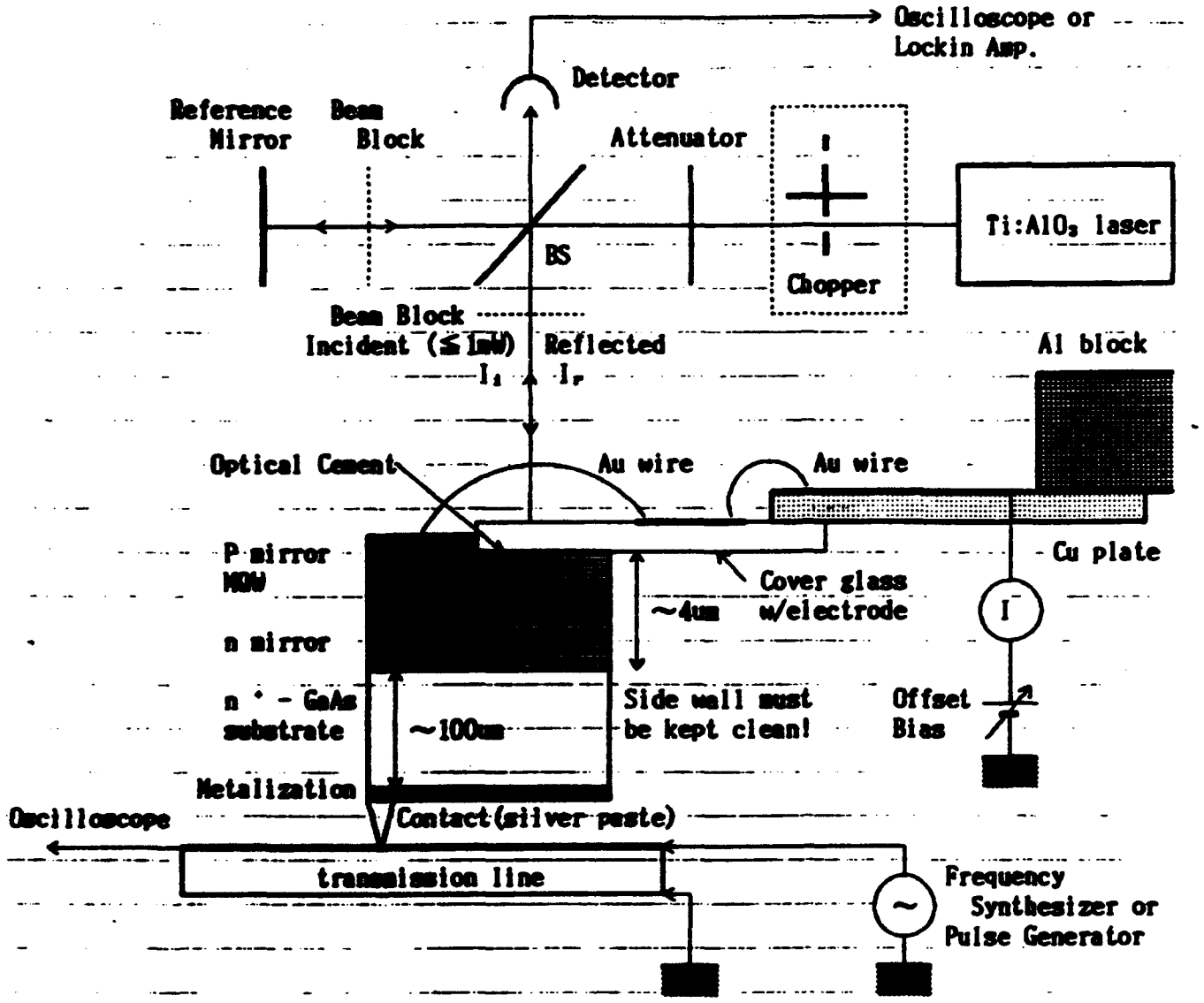

Fig. 9 High speed probing test set-up

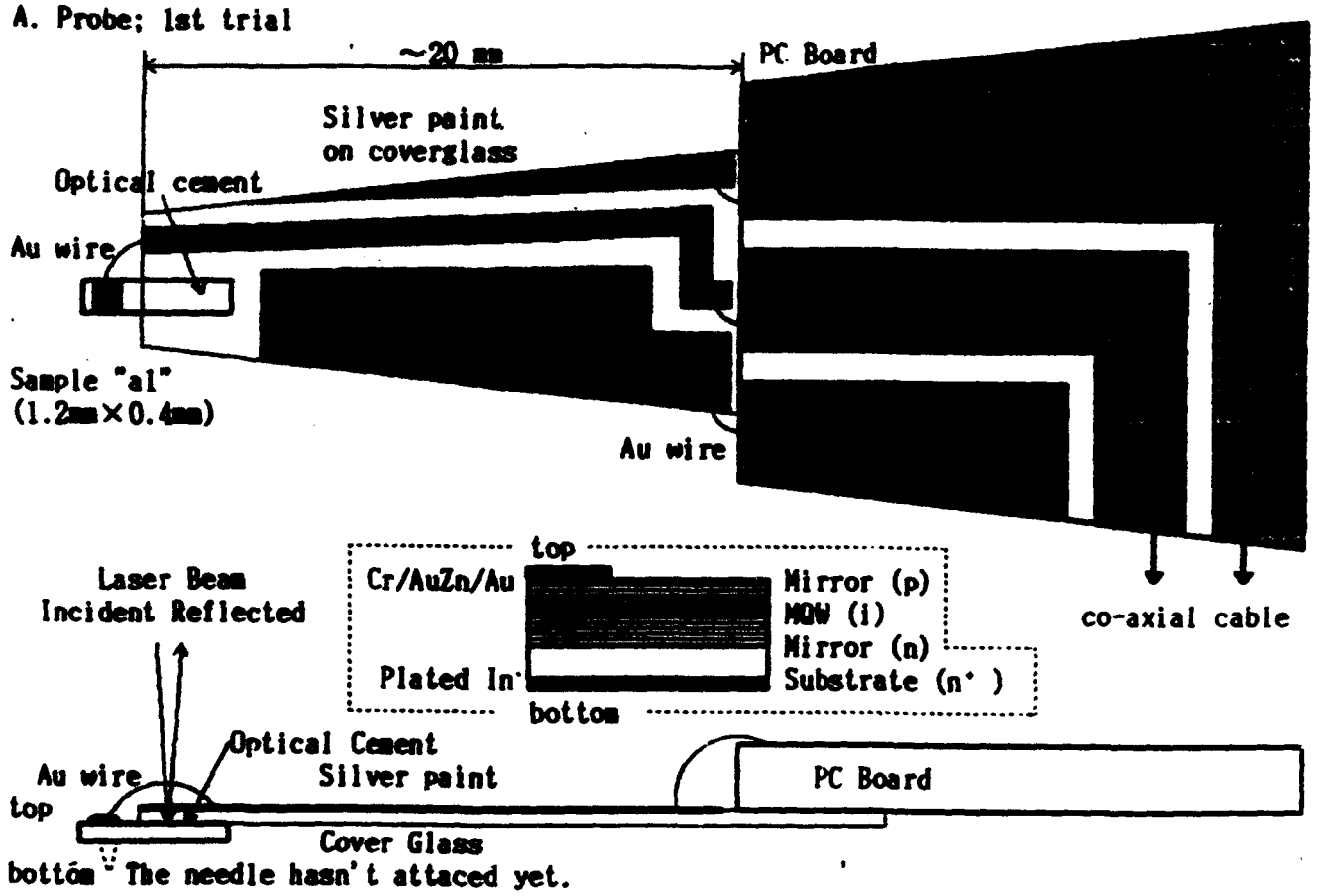

B. Set-up

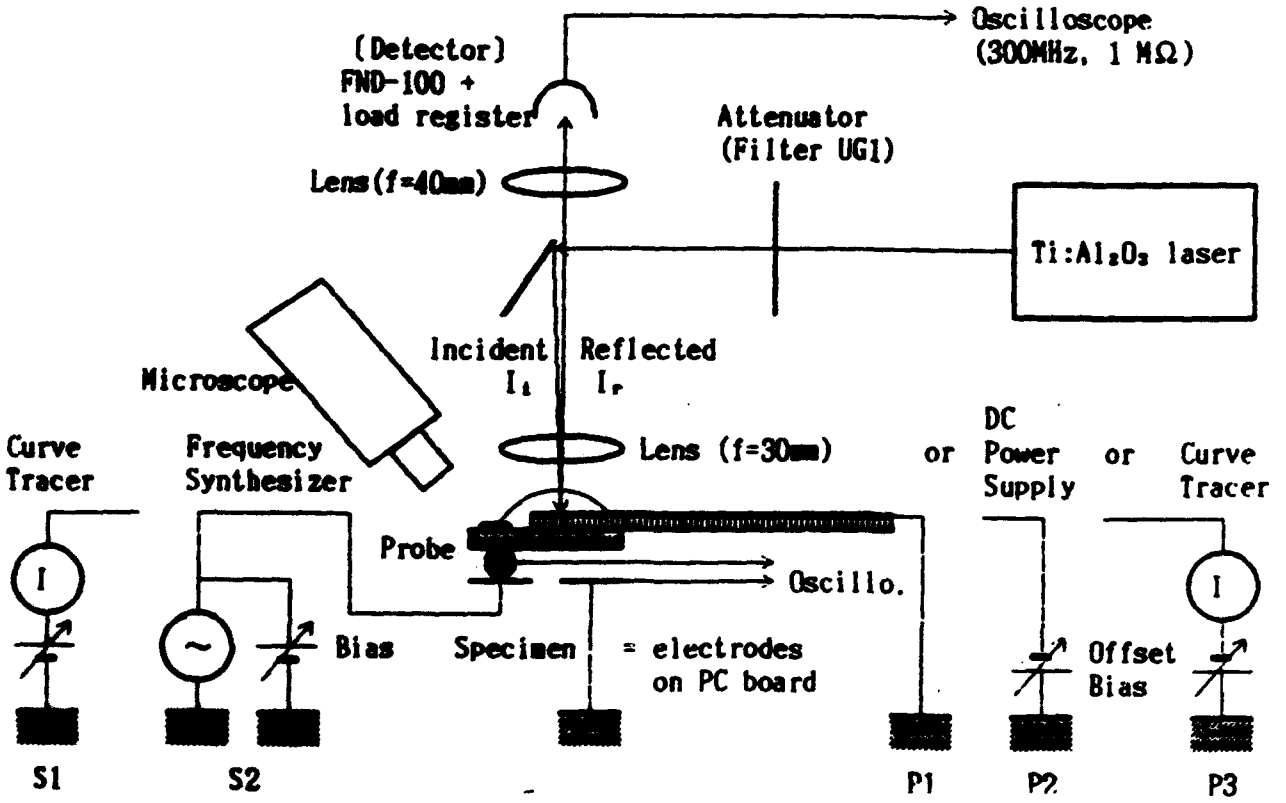

Fig. 10 Detailed view of sample structure and electrical set-up

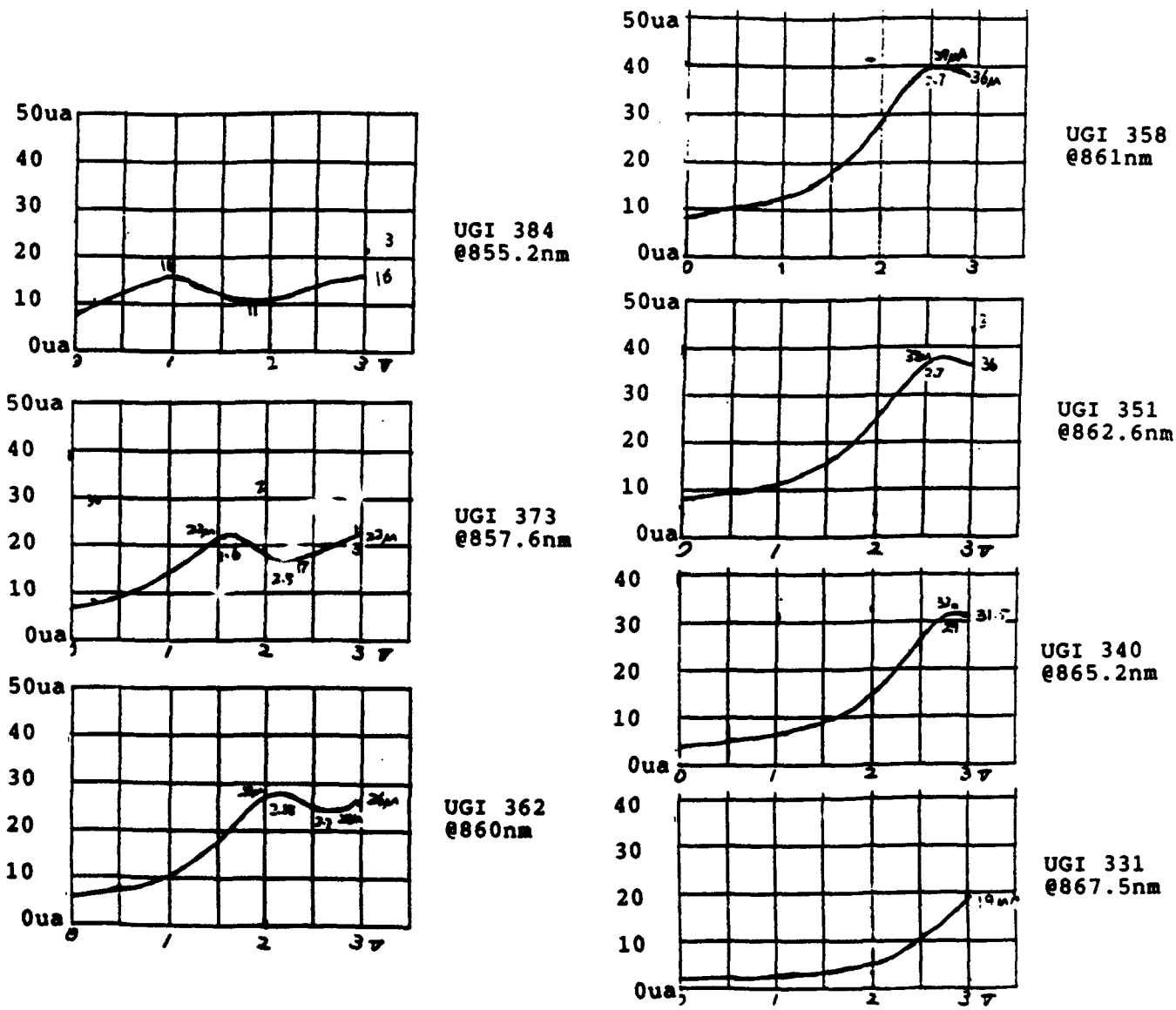

Fig. 11 I-V curves as a function of wavelength

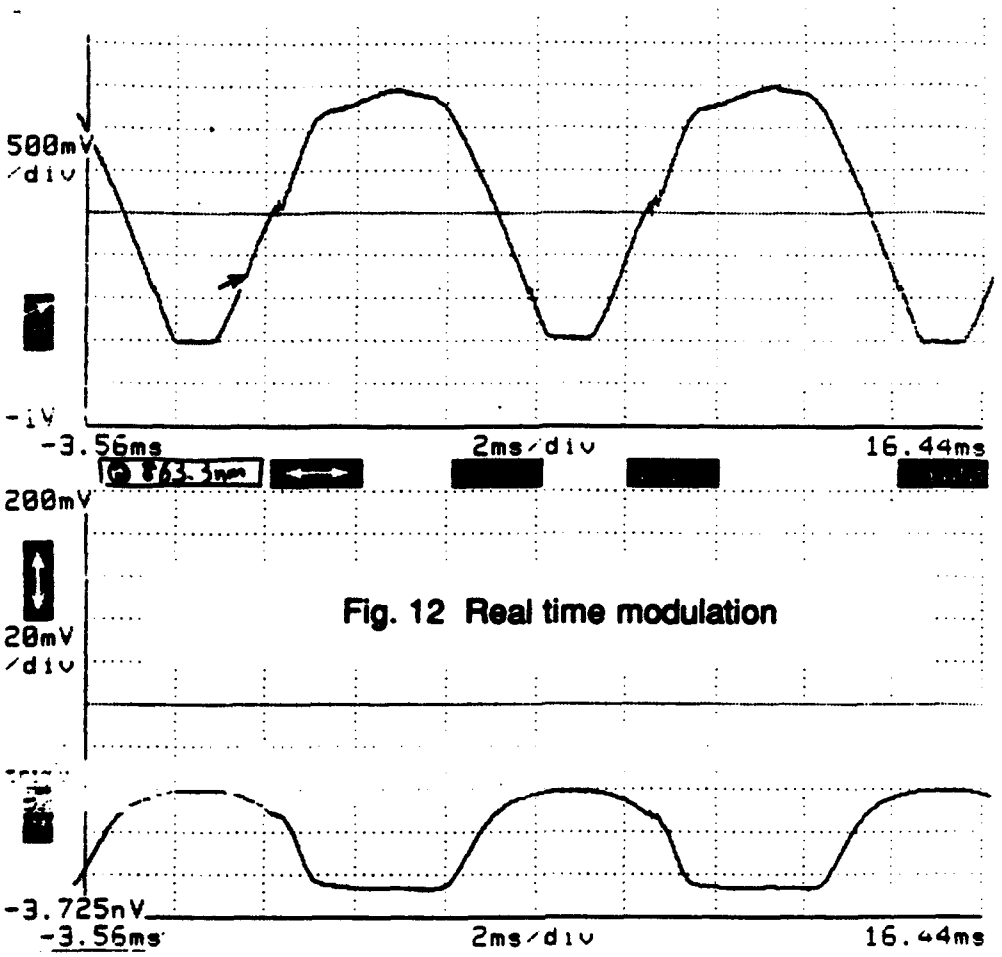

Fig. 12 Real time modulation

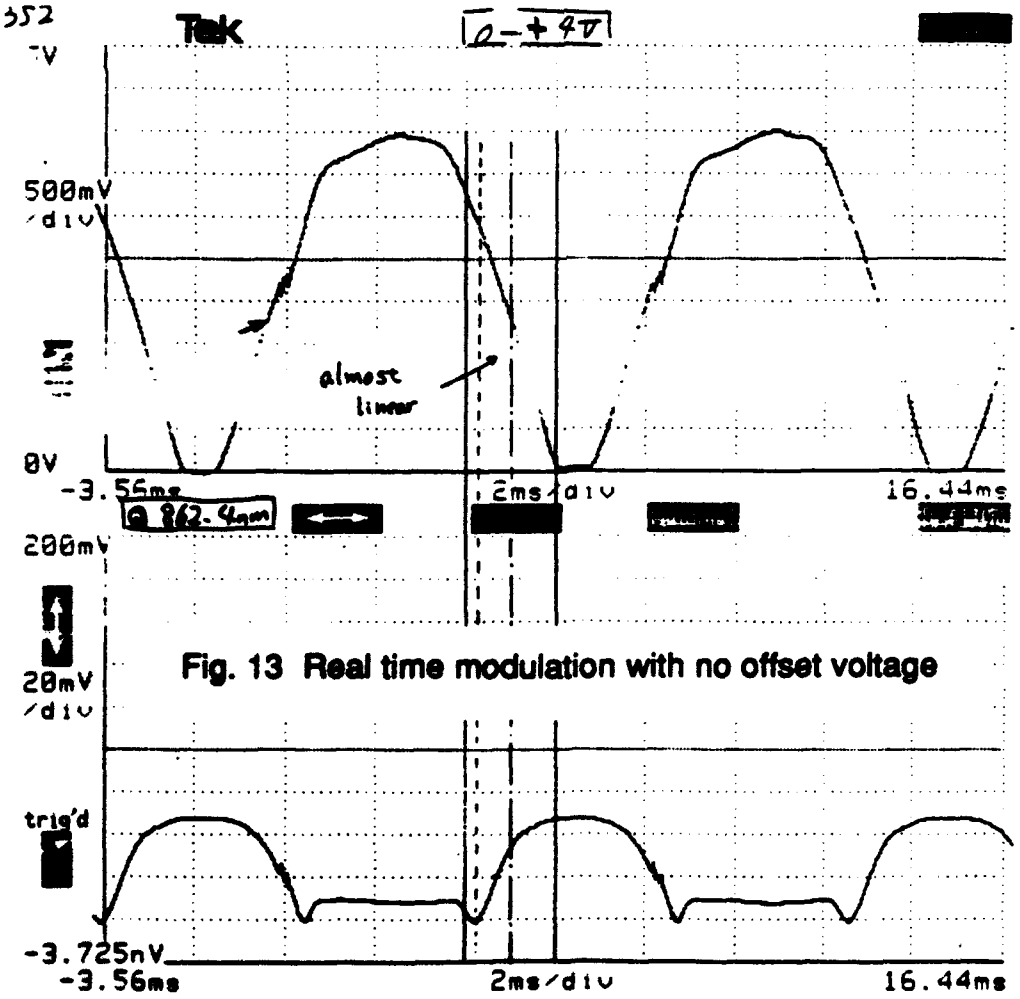

Fig. 13 Real time modulation with no offset voltage

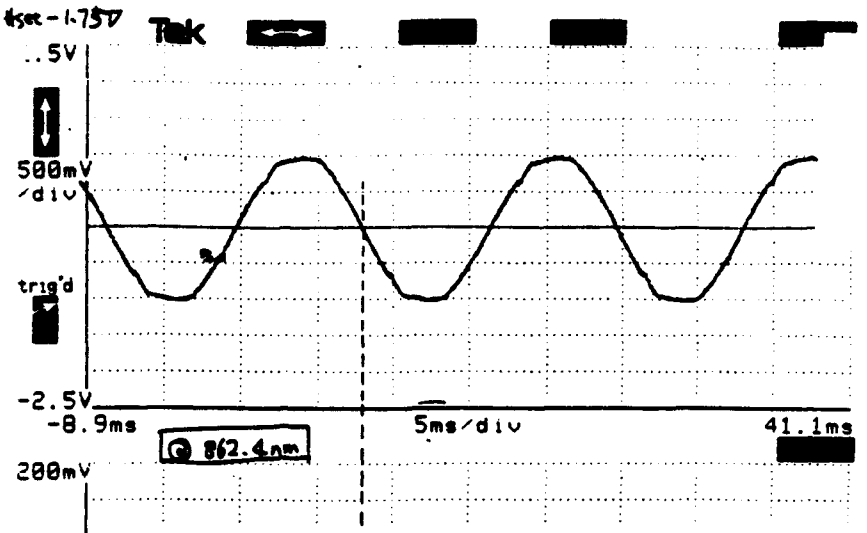

Fig. 14 Real time modulation with -1.75 V offset

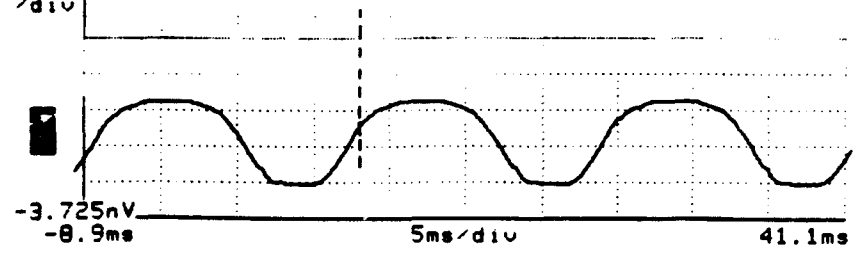

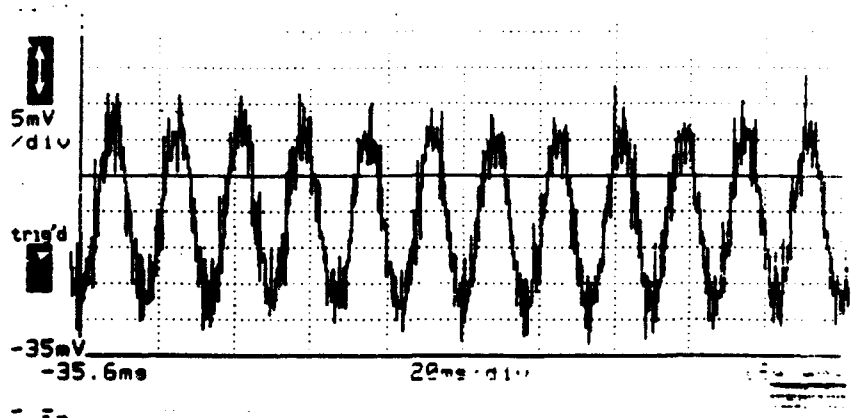

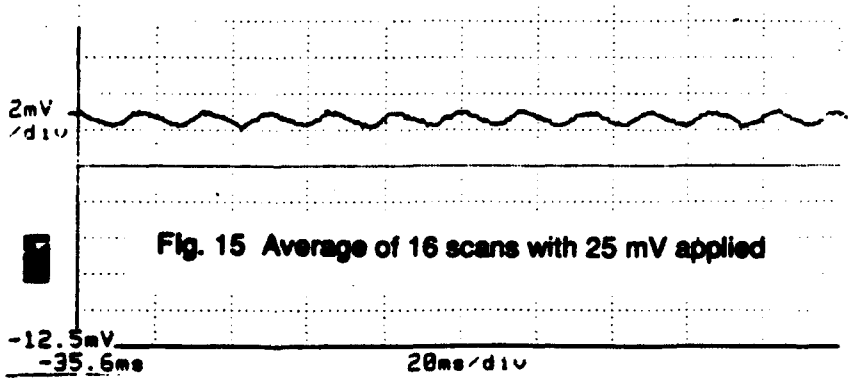

Fig. 15 Average of 16 scans with 25 mV applied

A. Set-up

a. MQW ASFP modulator

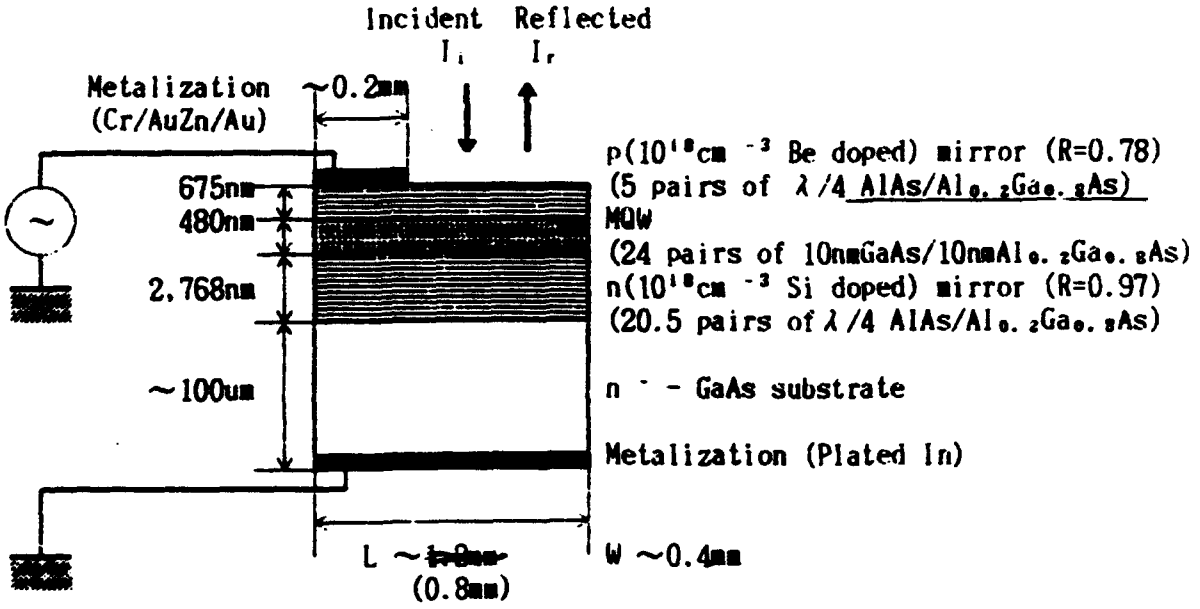

Fig. 16 More advanced modulator design

b. Test fixture

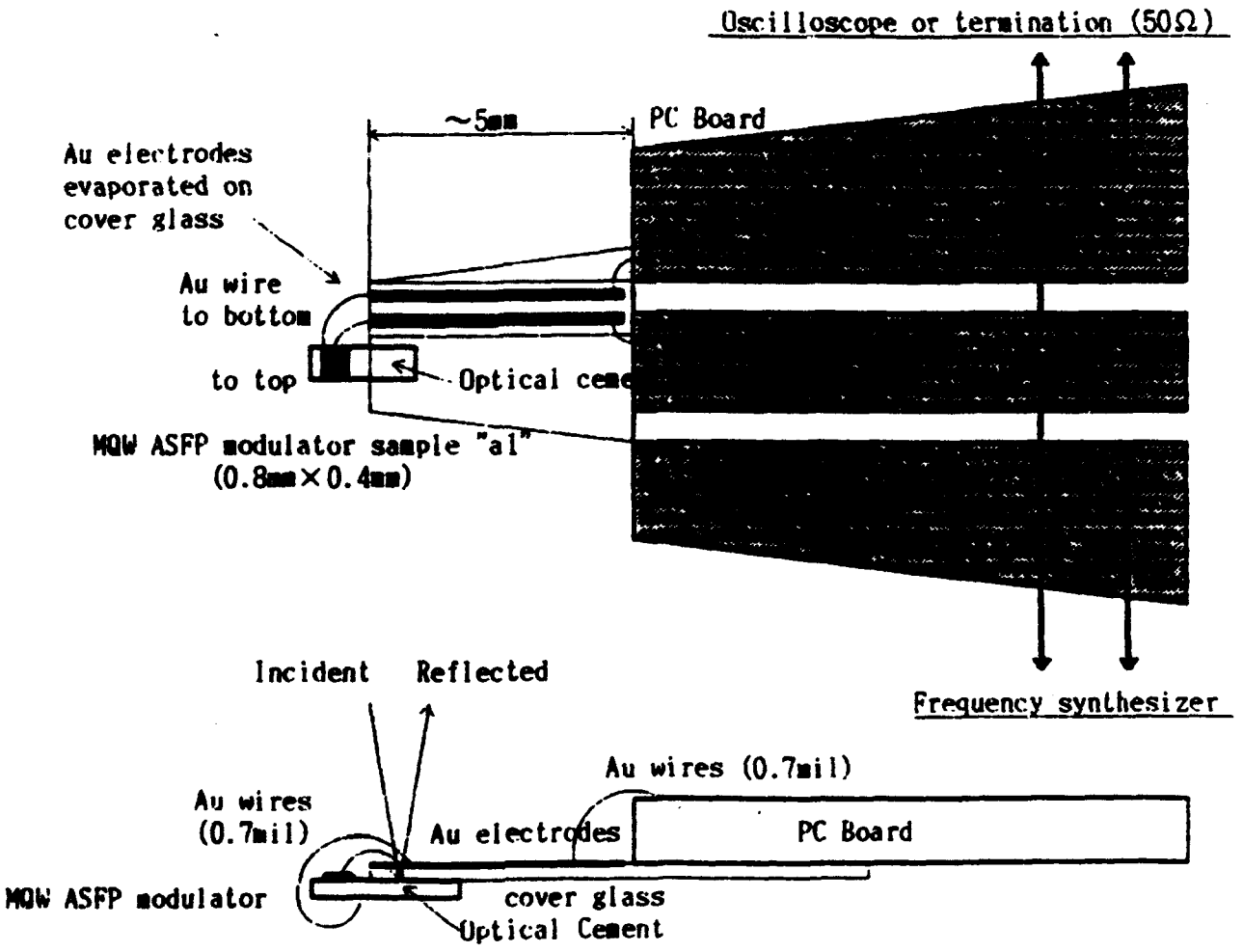

Fig. 17 More advanced probe design

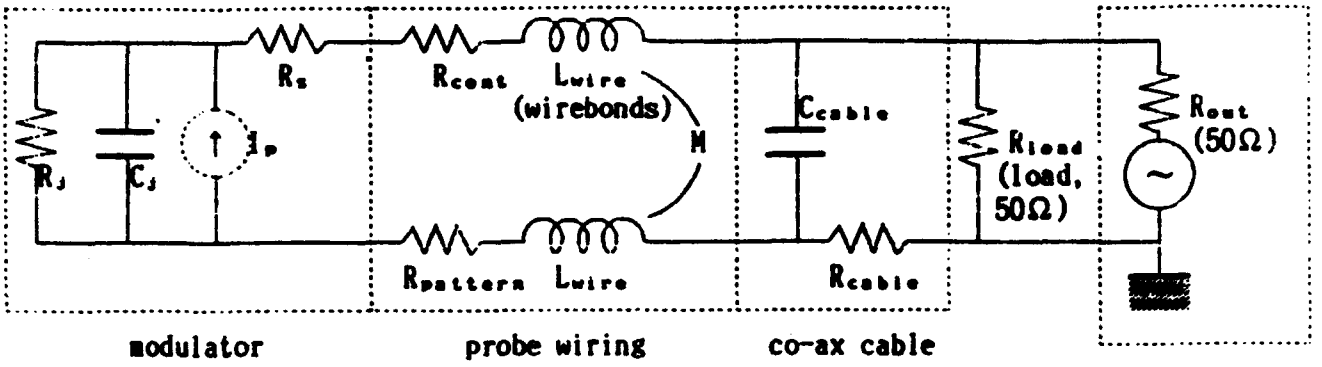

Fig. 18 Circuit model for probes

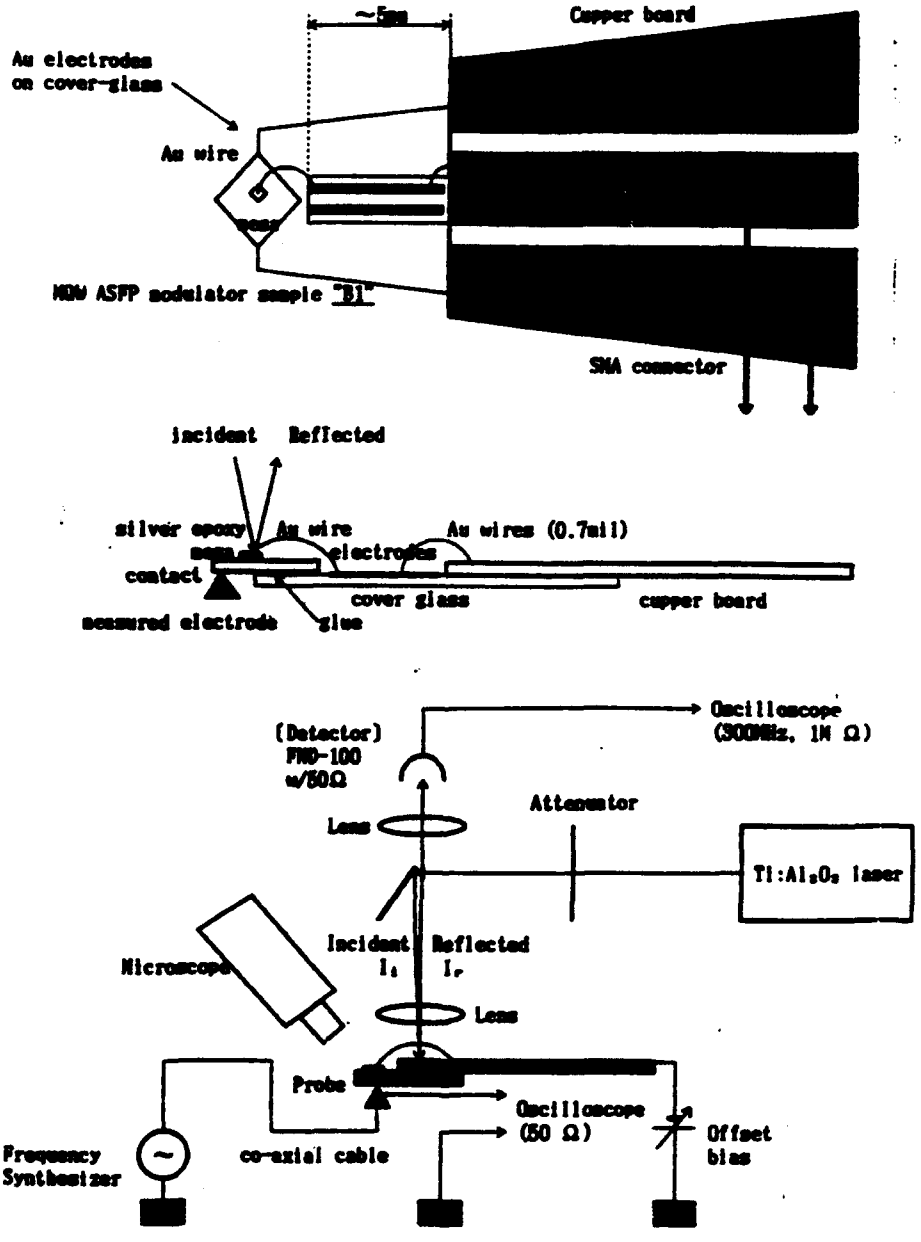

Fig. 19 Set-up for testing higher speed mesa structures

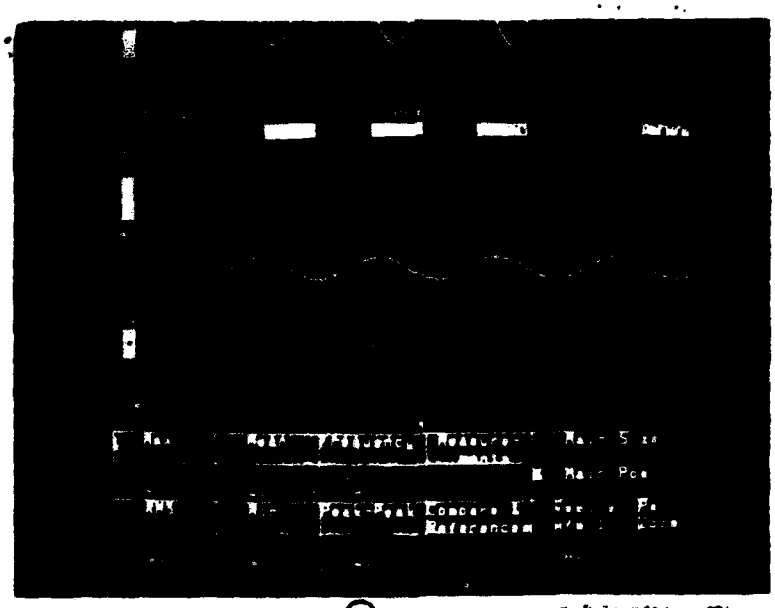

f=45MHz
p-p=1.040mv
vert: 1mv/div.
hor: 10ns/div.

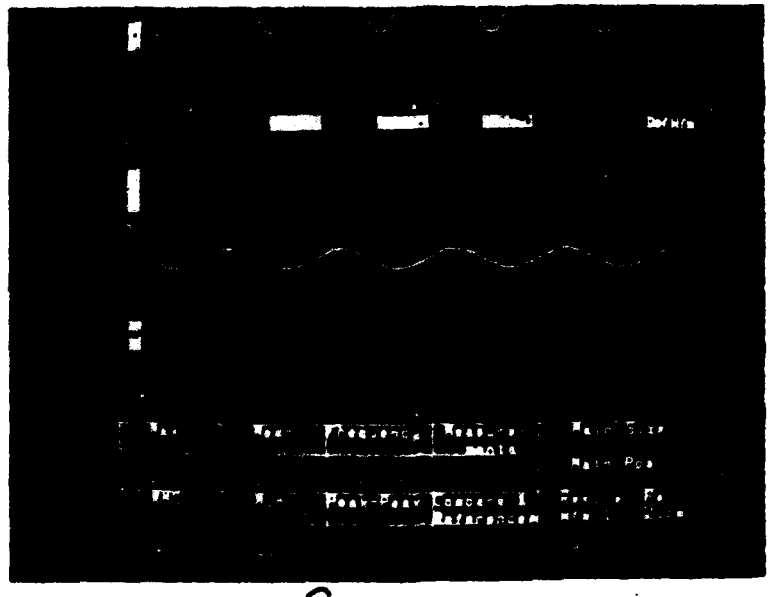

f=96MHz
p-p=0.912mv
vert: 1mv/div.
hor: 5ns/div.

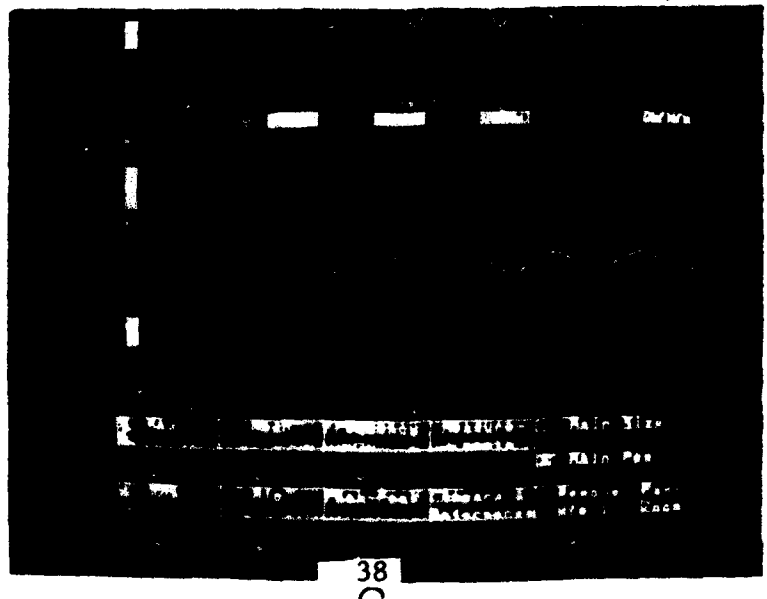

f=126MHz
p-p=0.870mv
vert: 1mv/div.
hor: 5ns/div.

Fig. 20 Experimental results of higher speed modulators

IV. Magnetic field probes

A. Theory of operation

This is a relatively new area of study for IC testing, but it represents another alternative that is completely non-contacting in nature. The work is only preliminary in nature, but is presented here to provide a more complete picture of the options that potentially exist.

The basic principle is one of interacting with the magnetic fields above a circuit [3] rather than the electric fields (as used for E-O sampling). By inserting a loop type probe into the fringing magnetic fields above a circuit, a current is induced that is proportional to the signal on the circuit lines. This current can then be sampled in the conventional photoconductive way. Thus P-C switching is used as the sampling gate but a non-contacting loop is the actual probe element.

The feasability of integrating a magnetic probe with a photoconductive sampling gate is evaluated. The theoretical coupling between a transmission line and the probe is first solved numerically. This result is then compared with the noise of a photoconductive switch. We show that the combination of magnetic field probe and photoconductive switch can remove the requirement of physical contact which is necessary in photoconductive sampling, but at the price of less sensitivity and lower dynamic range. The possibility of using this method in reverse, as a noncontact pulser, is also touched upon in this report.

In analyzing the magnetic probe, the circuit to be tested is represented by a coplanar strip line and the magnetic probe is a metal loop. The structure is shown in Fig.1. A TEM wave is assumed to be the only mode that can propagate on transmission line. Although this assumption is not reasonable at high frequency when the wavelength is comparable to the size of the transverse dimension of the strip line, it does give some quantitative estimations of the coupling efficiency between the strip line and the magnetic loop.

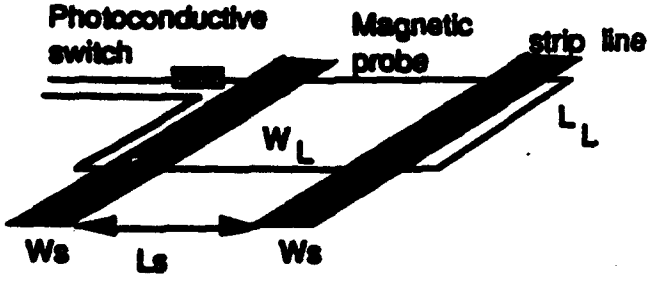

Fig.1 The magnetic probe & strip line

Because a TEM wave approximation is assumed, Maxwell's equations are reduced to a two-dimension Poisson's equation. It can be solved numerically by a finite difference method [4]. The entire procedure is summarized as

1. TEM wave assumption => Poisson's equation
2. Discretize the Poisson's eq. with finite difference method
3. Solve the coupled linear equations by over-relaxation method
4. Get the field distribution around strip line
5. Calculating the coupling coefficient

The coupling coefficient is defined as the percentage of magnetic flux which generated on the strip line and is coupled into the magnetic probe.

After calculating the coupling coefficient, it is found that the larger loop width dose not mean better coupling efficiency. Fig.2 shows the coupling coefficient for three different loop widths. The best one has a loop width just equal to the sum of the separation of the strip line and the strip line width (Ls+Ws). The reason why there is a optimal loop width can be understood from the field distribution in Fig.2. If we keep the loop width smaller than optimum size (30 μm in this case). The smaller the loop is, the fewer magnetic flux lines can go into the loop. However, if the width increases over the optimal size, some magnetic flux at the edge of the loop points downward, instead of all the flux pointing upward. Therefore, the cancelation between magnetic flux occurs and the coupling efficiency is reduced. Because the optimum width is only a little better than the other two cases, we conclude that the width of the loop is not a very sensitive factor as long as it stays around the same size as the separation between the strip lines.

The other interesting effect is how the separation between strip lines affects the coupling coefficient. Fig.3a shows the coupling coefficient of two strip line separations, where the optimal loop width is used in both cases. It is found that the larger the separation is, the better the coupling coefficient will be. This can also be understood from the field distribution in Fig.3b. If the separation of strip lines is smaller, the curvature of magnetic flux will be large.and less signal will be coupled to the loop. Therefore, when the loop moves away from the strip line, the coupling coefficient of the smaller strip line will decrease faster.

Figure 4 shows how the miss-alignment will degrade the coupling coefficient. If the magnetic probe moves laterally to one side, the signal will be reduced to zero and then it will increasing again. The zero occurred when the center of the magnetic probe is just over the center of either the strip line.

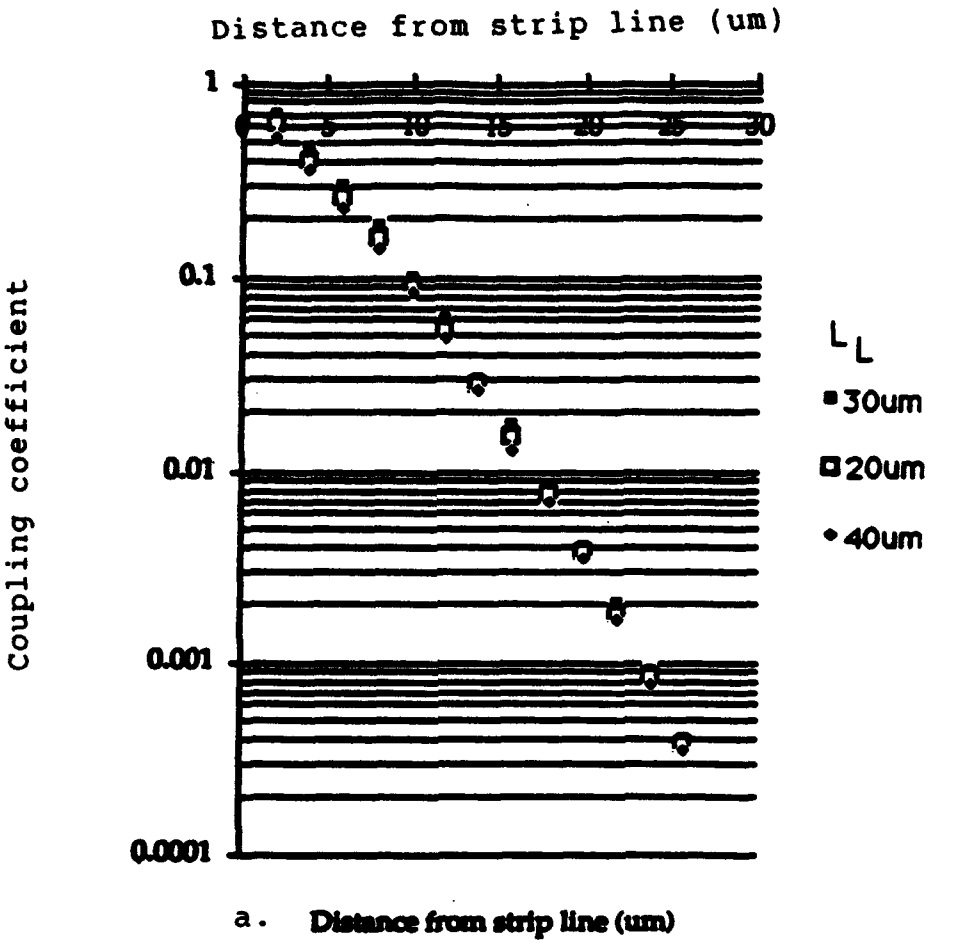

Fig. 2 Magnetic coupling to loops versus distance and size

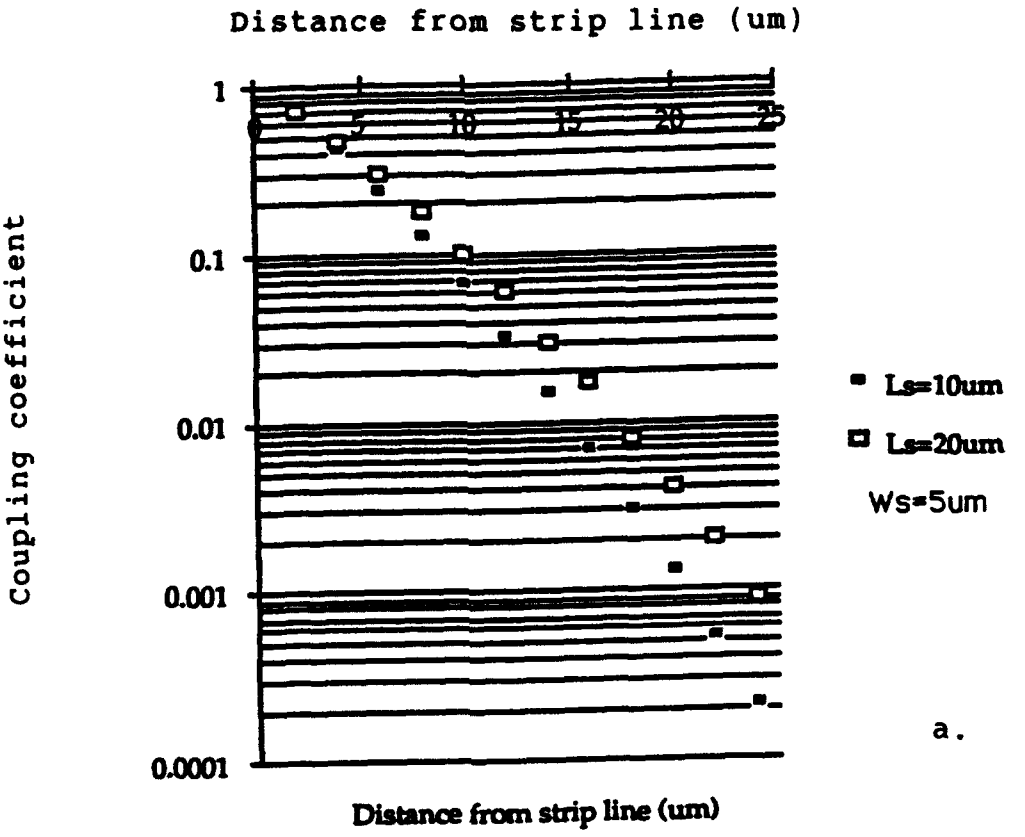

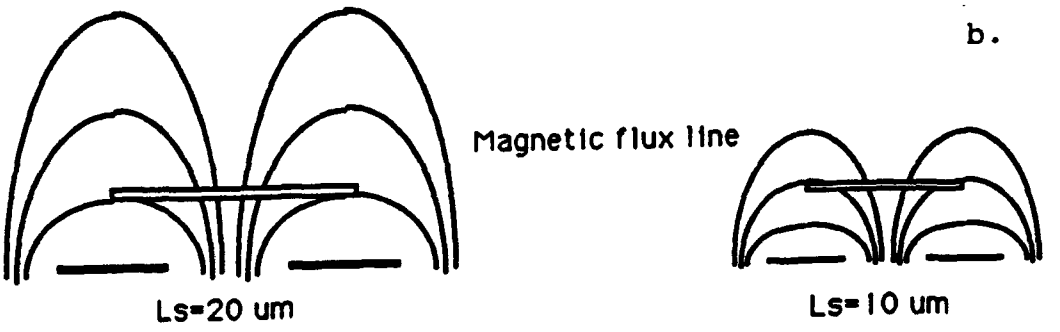

Fig. 3 Magnetic coupling to loops versus line separation

Fig. 4 Effect of lateral misalignment

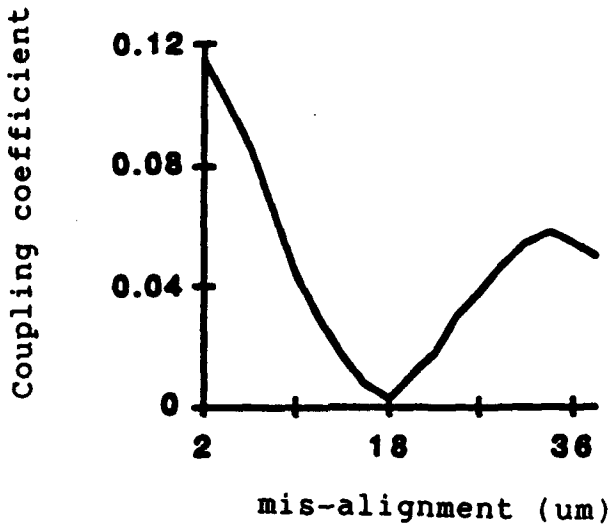

Figure.4

B. Temporal response

The length of the loop (L_L) and the speed of photoconductive switch determine the time resolution of the probe. Since the electric signals on the strip lines travel at the speed of 10^{14} μm/sec, for a 1 ps sampling time duration, the signals have already traveled for 100 μm. But for a sinusoidal signal, there should be at least two sampling points per cycle. Therefore, the minimum wavelength of electric signals on the strip lines is 200 μm which is equivalent to a frequency of 500 GHz.

The length of the loop should be much less than the wavelength of the electric signal. Otherwise, the cancelation of magnetic flux in the loop will occur and the assumption of quasi-static will break. But a small loop area also degrades the sensitivity, thus the length of the loop should be kept at a reasonable number. For the above case, 30 μm is a reasonable choice.

Since all the dimensions must be kept in small compared with the wavelength, the induced voltage on the loop can be considered as a quasi-static case. For a 5V photoconductively generated pulse with a 5 ps rising time and with a 10% strip lines to probe coupling efficiency. The signal induced on the loop is 10 mV, from Faraday's law. Therefore, the noise level of our photoconductive switch should be less than this figure, or the signal will not be detectable.

Strip lines parameter: Ls=20 μm, Ws=10 μm

Loop size: 30 μm x 30 μm

Total magnetic flux on the loop at the end of switching:

$$\Psi = 10\% \times 5V \times 30\ \mu m / (3\times10^{14}\ \mu m/sec) = 5\times10^{-14}\ V\ sec$$

Induced loop voltage: $V = (-d\Psi / dt) = 5\times10^{-14}\ V\ sec / 5\ ps = 10\ mV$

The experimental setup is shown in Fig. 5. A 200 MHz square wave signal is fed into the strip line. This signal is sampled by a photoconductive switch and then detected by a lock-in amplifier. The output signal of the lock-in amplifier is proportional to the input signal amplitude on the strip line. The measurement result of this setup is shown in Fig. 6. The input signal amplitude in the right hand side of Fig.8 is larger than that in the left hand side by 1 mV. This step voltage difference is used as a reference level to know the noise amplitude. From this measurement, the noise associate with the photoconductive sampling gate is around 0.8 mV

For a magnetic probe, it transfers the alternating magnetic field generated by a waveform on strip lines to a signal voltage. In order to detect the waveform, the signal voltage on the magnetic probe should be larger than the noise level. From the numerical example in the last section, the signal voltage is around 10 mV. This figure is larger than the noise level, so the combination of magnetic probe with photoconducting sampling gate is feasible but with poor signal noise ratio.

C. IDEA OF SIGNAL INJECTOR

There is a unique characteristic of magnetic probe, that is, it can be used as a signal injector. Because the magnetic flux coupling is mutual for both probe and loop, if we reverse the role of field generation (strip line) and field detection (loop probe), we can use magnetic probe to inject the signal into a strip line. Furthermore, since the injected signal is just related to the time derivative of the magnetic flux change (Faraday's law), even a slow photoconductive switch can generate a electric pulse whose duration is much shorter than the carrier lifetime in that slow photoconductive switch. Therefore, this method offers an interesting way to inject fast electrical signals into a transmission lines without needing contact to the dc bias wires and "in situ" photoconductive switch. This will be another application of a magnetic probe with a phtoconductive switch.

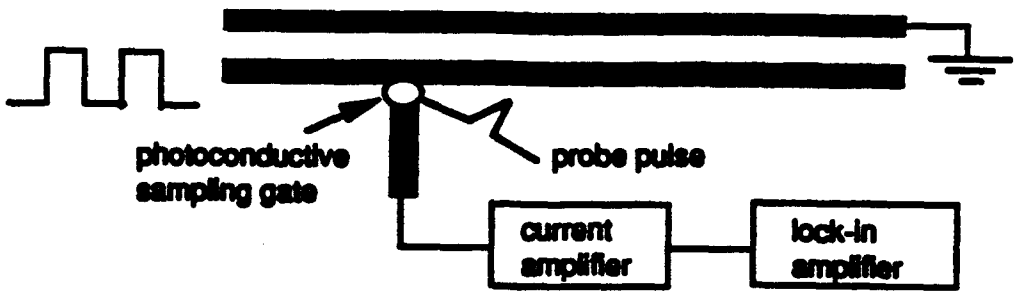

Fig. 5 Experimental sensitivity set-up

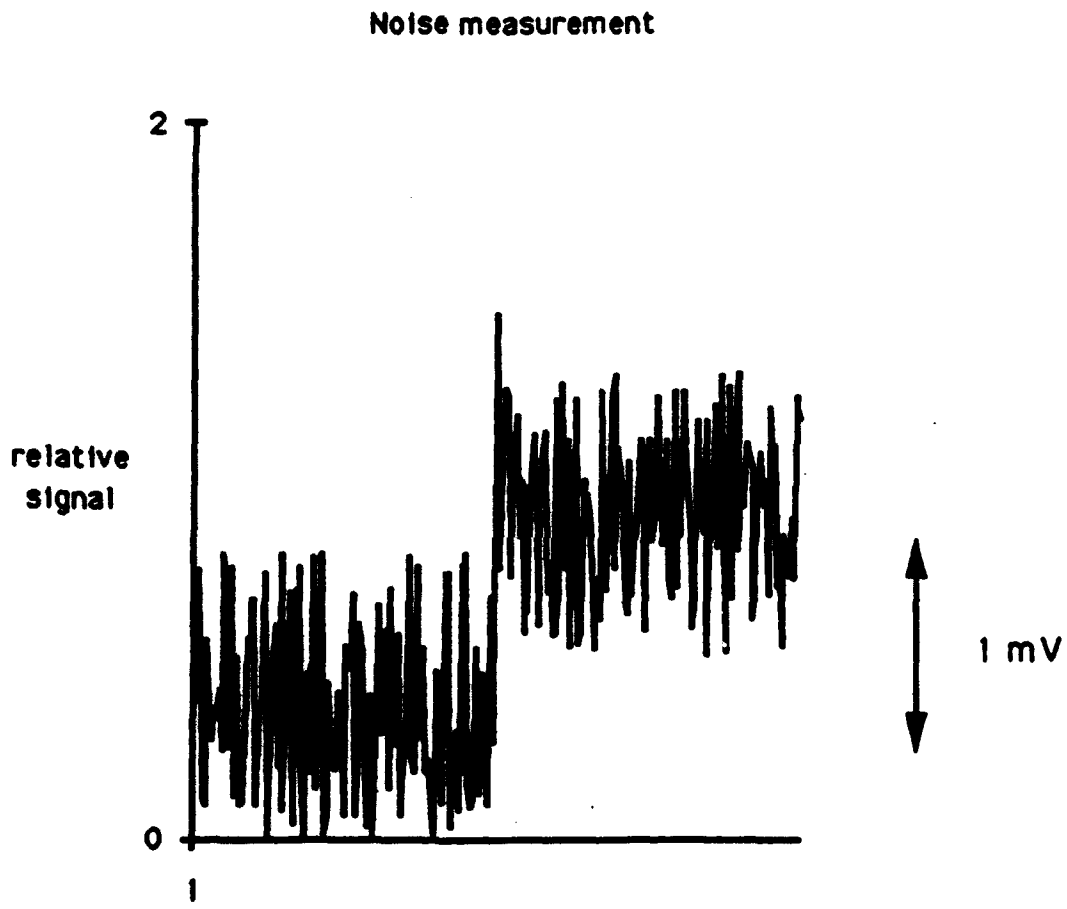

Fig. 6 Minimum detectable signal result

D. CONCLUSION

It is feasible to use a magnetic probe with a photoconductive sampling gate, which removes the requirement of "in situ" photoconductive gates for optoelectronic sampling. However, this is accomplished at the price of lower sensitivity and smaller dynamic range. For signal injector, the combination of magnetic probe and photoconductive switch offer a unique non-contact way to generate short electric pulses in transmission lines.

V. Photoconductive probes

Some very preliminary data on the use of photoconductive, contacting probes was obtained. The basic principle is the same as for conventional photoconductive sampling where the P-C sampling gate is integrated on the surface of the circuit under study (see work by Auston et al., ref. [1]). It has been shown by many workers that this technique, when used at ns time scales, is far more sensitive than any electro-optic technique. This is because charge is physically removed from the circuit under study by the sampling gate, and immediately detected by very sensitive current pre-amplifiers. Signals in μV level can be easily measured.

Our desire was to implement this type of sampling gate as an external probe that could be positioned anywhere along a circuit line. A very sharp tip would make contact with the line and the sampling gate would be positioned as close to the tip as possible so as to provide as small a perturbation to the circuit as possible. Our hope was that this would provide a very sensitive probe that would still not be too perturbative for time scales in the ns range, where the tip and gate could still be considered a lumped element and charge would be sampled for only picoseconds.

Our only experiment consisted of making a special probe by bonding a standard tungsten probe tip to the input side of a GaAs photoconductive switch as shown in Fig. 1, which was then gated by pulses from a CPM laser. The gating time of the GaAs sample used was about 100 ps, which would be ideally suited to the speeds being considered in this work. Sensitivity should be more than adequate.

Figure 2 shows the measured waveform of a ±100 mV sine wave at 100 MHz, and Fig. 3 shows that even a 1 mV signal can be resolved. Fig. 4 shows that the overall frequency response of even this very crude probe goes easily out to 500 MHz.

The sensitivity and speed of this type of probe are ideal for the application at hand, however it will remain to be seen whether a contacting probe could be designed for this type of use. This would be a very good direction to pursue work. We should not rule out contacting type probes just because existing technology does not meet the current needs. One could envision a highly compact probe tip with an integrated P-C switch and fiber light delivery system that could be implemented on existing probe stations with ease.

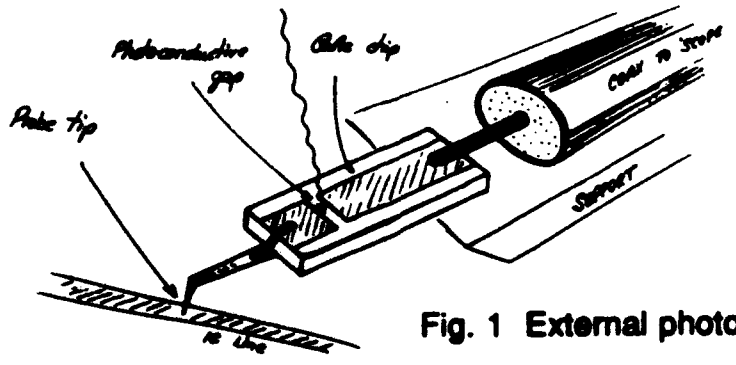

Fig. 1 External photoconductive gated probe

Fig. 2 Measurement of 100 mV, 100 MHz signal

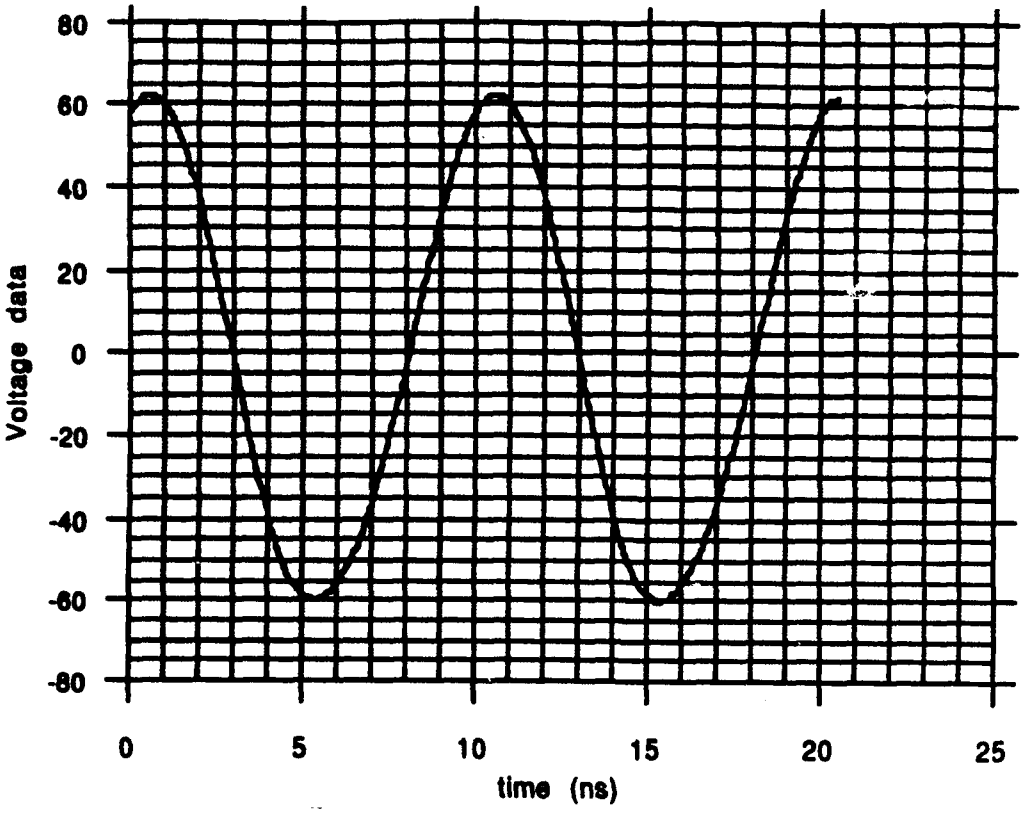

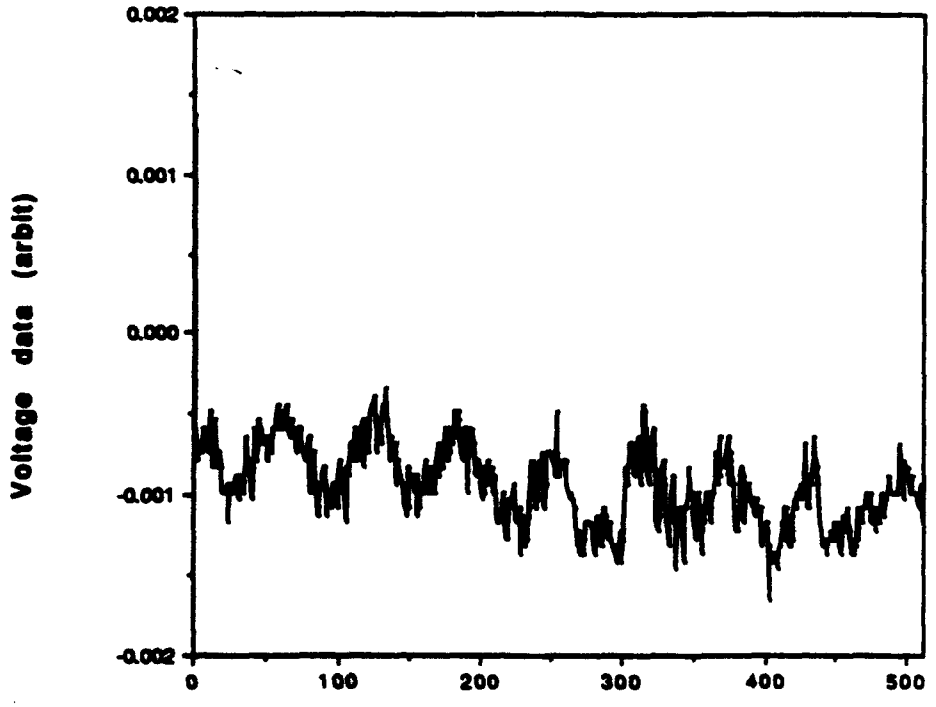

Fig. 3 Measurement of 1 mV, 100 MHz signal

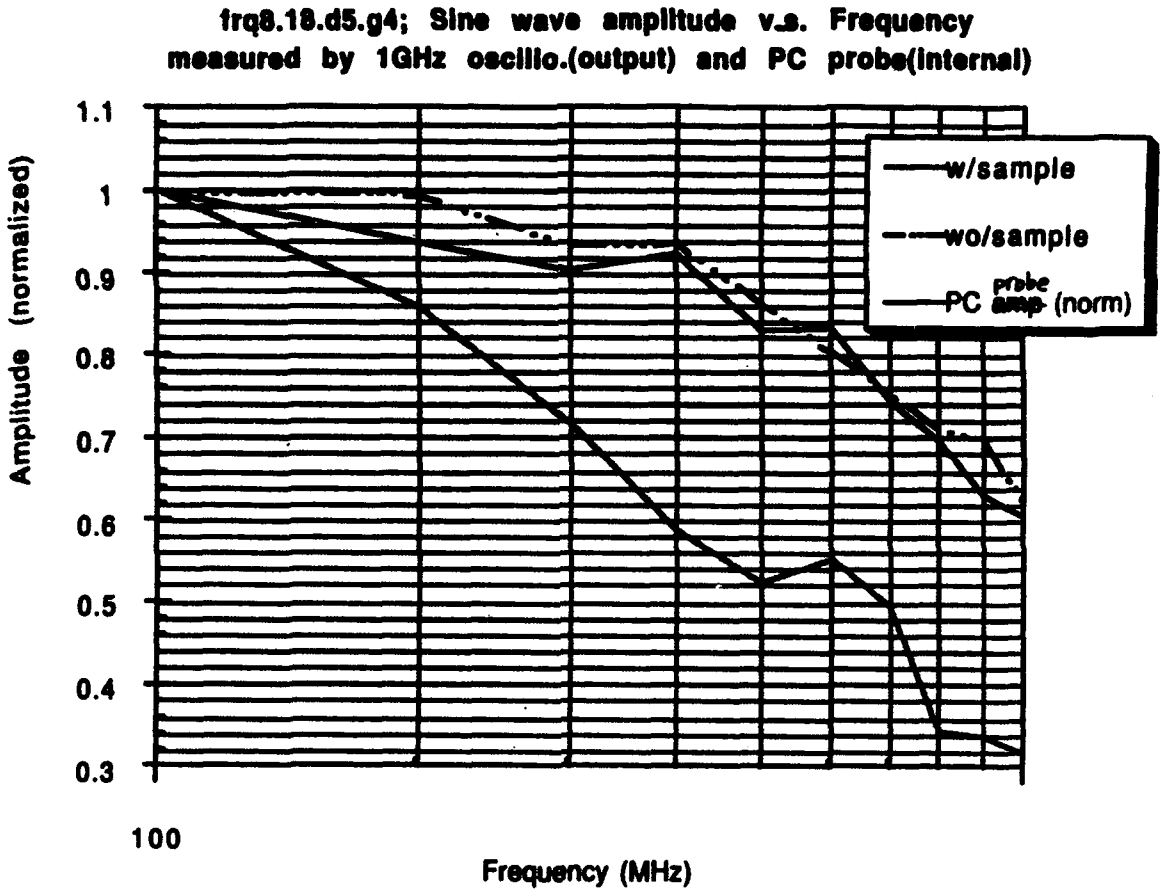

Fig. 4 Overall frequency response of photoconductive probe

VI. Summary of findings

We have looked at four types of optical modulator/ transducer/ gate that would be suitable for use in an internal node probe for VLSI integrated circuits. The operational specifications we attempted to achieve were: ≤50 mV real time sensitivity, ≤5 ns temporal response, and ≤2 μm spatial resolution.

Bulk lithium tantalate Fabry-Perot modulators are highly unlikely candidates for these applications. The needed real time sensitivity would be very difficult to achieve in light of the fabrication constraints that would have to be imposed. The fact that they could be non-contacting is a mute point.

MQW electro-absorption modulators show adequate sensitivity, but also are highly non-linear and generate a significant photo-current that could be perturbing to the circuit under study. A possible solution to this problem would be the use of electro-refractive, phase only modulators which do not absorb any light and hence exhibit no photo-current. They are slightly less sensitive, but have an increased dynamic range. These type modulators also need contact with the circuit.

Magnetic loop probes are novel, non-contacting probes that can function both as signal samplers and injectors. Initial tests indicate that spatial resolution would be poor, and sensitivity would not be adequate in the form they are now used. There is still work to be done here.

Photoconductive sampling probes appear to be the most promising candidates in all catagories. Sensitivity is extremely high, and the speed of response can be tailored to suit the particular needs of the circuit under study. The traditional drawback is the need to contact the circuit. However, this is an area of technology that has not been pushed to the limits yet. Other workers have already demostrated the fabrication of sub-micron sized metal points for totally different applications. Furthermore, much work is currently going on to enhance the sensitivity of photoconductive detectors [5] used as gates and switches (under AFOSR contracts). Combining these tip and gate technologies could hold great promise for IC testing in the future. Of all the above techniques, this one appears to be the most interesting.

VII. Acknowledgements

This work was performed by several scientists and students working both together and independently. Their efforts are deeply appreciated. Credit is due as follows:

- K. Ozaki, visiting scientist, Fujitsu Labs: F-P, MQW, and P-C modulators
- J-W. Kim, GSRA: F-P modulator
- H-J. Cheng, GSRA: magnetic probe
- J.V. Rudd, GSRA: laser systems

VIII. References

[1] See e.g. "Measurement of high-speed signals in solid state devices," R.B. Marcus, ed., Academic Press, 1990.

[2] R.H. Yan, R.J. Simes, and L.A. Coldren, "Extremely low-voltage Fabry-Perot reflection modulators," IEEE Phot. Tech. Lett., 2(2), 118, Feb. 1990.

[3] S. Osofsky, "A non-contact probe for measurements on high frequency planar circuits," IEEE MTT-S Digest, 1989.

[4] W.C. Johnson, "Transmission lines and networks," McGraw-Hill, New York, 1950.

[5] Y. Chen, S. Williamson, T. Brock, F.W. Smith, and A.R. Calawa, "375 GHz bandwidth photoconductive detector," APL 59 (16), 1984, Oct 1991, and

Y. Chen, S. Williamson, T. Brock, F.W. Smith, and A.R. Calawa, "Integrated high-sensitivity photodetector and correlator with picosecond resolution," to be presented at Int. Elec. Dev. Mtg., Washington D.C., Dec. 1991.